Universidade de Aveiro Departamento de Química
2010

Vanda Filipa Silva Fernandes

Characterization of biodiesels produced from mixtures of vegetable oils

Caracterização de biodieseis produzidos a partir de misturas de óleos vegetais

Universidade de Aveiro Departamento de Química
2010

Vanda Filipa Silva Fernandes

Characterization of biodiesels produced from mixtures of vegetable oils

Caracterização de biodieseis produzidos a partir de misturas de óleos vegetais

Dissertação apresentada à Universidade de Aveiro para cumprimento dos requisitos necessários à obtenção do grau de Mestre em Engenharia Química, realizada sob a orientação científica do Dr. João Araújo Pereira Coutinho, Professor Associado do Departamento de Química da Universidade de Aveiro.

Dedico este trabalho aos meus pais…

o júri

presidente

Professora Doutora Maria Inês Purcell de Portugal Branco
Professora auxiliar do Departamento de Química da Universidade de Aveiro

Professor Doutor João Manuel da Costa e Araújo Pereira Coutinho
Professor associado com agregação do Departamento de Química da Universidade de Aveiro

Professora Doutora Sílvia Maria Carriço Santos Monteiro
Professora adjunta do Departamento de Engenharia do Ambiente do Instituto Politécnico de Leiria

agradecimentos

Ao meu orientador, Doutor João A. P. Coutinho, por me ter aceite sob a sua orientação, pelo conhecimento transmitido, pela paciência e disponibilidade que sempre demonstrou.

Agradeço também à Sandra Magina que me auxiliou na parte das análises de DSC.

Ao grupo Path, que é sem dúvida em excelente grupo para trabalhar!
À Maria Jorge, pela orientação que me deu, pelos ensinamentos transmitidos, pela paciência e disponibilidade…sei que às vezes era muito chatinha! À Marise pela passagem de testemunho e ajuda inicial no laboratório! Ao Pedro, a Catarina Neves e Catarina Varanda pela sua sempre disponibilidade em ajudar no laboratório sempre que precisava! Ao meu grupinho dos almoços, jantares e às vezes noitadas no laboratório….obrigado pelos momentos divertidos, pelo apoio e disponibilidade que sempre demonstraram!

Aos meus amigos que me acompanharam ao longo desta longa jornada em Aveiro, obrigado por me terem aturado e foi um gosto muito grande ter partilhado este caminho com todos vocês!

À minha siamesa, Marta, por tudo o que passamos nestes 4 anitos, por estares sempre presente, pela paciência, por aturares o meu mau humor…e espero sinceramente que me continues a aturar pelos próximos anos, apesar do futuro incerto…!

Aos meus amigos de longa data de Mangualde, que apesar de mais distantes sempre estiveram presentes quando precisei! Fico contente por saber que o tempo não nos afastou!

Aos meus pais por me terem dado esta oportunidade e as minhas maninhas! Obrigado a todos por estarem sempre presentes, por acreditarem que sou capaz, pelo apoio em todos os momentos! Sem vocês isto teria sido mais complicado!

Muito obrigado a todos!

Palavras-chave: Biodiesel, Diesel fuel, Propriedades termofísicas, Desempenho das misturas, Regra das misturas, Desempenho a baixas temperaturas, Equilíbrio Sólido-Líquido, Modelação, UNIQUAC Preditivo.

Resumo: Nos últimos anos o biodiesel tem recebido uma atenção notável devido à sua capacidade de substituir os combustíveis fósseis. É considerado um amigo do ambiente, devido às suas imensas vantagens. Este biocombustível é obtido a partir de recursos renováveis, portanto é considerado biodegradável, CO_2-neutro, não-tóxico e reduz significativamente as emissões gasosas com efeito de estufa.

É composto por uma mistura de ésteres mono alquílicos obtidos a partir de óleos vegetais, tais como, o óleo de soja, óleo de jatropha, óleo de colza, óleo de palma, óleo de girassol ou a partir de outras fontes como a gordura animal (sebo, banha), restos de óleo e gorduras de cozinha. O processo mais comum para a sua produção é através de uma reacção de transesterificação, onde o óleo vegetal reage com um álcool de cadeia curta na presença de um catalisador.

Devido às suas propriedades muito semelhantes ao diesel, são mutuamente miscíveis e assim podem ser misturados em qualquer proporção em ordem a melhorar as suas qualidades. O conhecimento das suas propriedades termofísicas como a densidade e viscosidade, que são afectadas pela temperatura, são muito importantes para a indústria automóvel.

Contudo, o biodiesel apresenta algumas desvantagens como elevada densidade, viscosidade, ponto de turvação e escoamento/fluxação em comparação com diesel fuel.

O seu comportamento a baixas temperaturas limita a sua aplicação em climas frios, sendo que este comportamento é influenciado pelas matérias-primas e álcool utilizado no processo de produção. Os biodieseis obtidos a partir de óleos com grande teor de ácidos gordos saturados induzem a um pior desempenho a baixas temperaturas, visto que são compostos sólidos a temperaturas mais baixas.

Neste trabalho, misturas binárias e ternárias de biodiesel de soja, colza e palma, e diesel fuel foram preparadas e medidas as suas viscosidades dinâmicas e densidade em função da temperatura. Para prever as densidades e viscosidades a partir dos compostos puros são utilizadas regras de mistura.

O comportamento a baixas temperaturas dos três biodieseis foi estudado. Onde a composição da fase líquida e sólida e a fracção de sólidos a temperaturas abaixo do ponto de turvação foram analisadas. Aplicou-se um modelo termodinâmico para descrever estes sistemas multifásicos e outros sistemas idênticos. Duas versões do modelo preditivo UNIQUAC, juntamente com uma abordagem que assume uma completa miscibilidade dos componentes na fase sólida, são avaliados em relação aos dados de equilíbrio de fases experimentais medidos.

.

Keywords: Biodiesel, Diesel fuel, Thermophysical properties, Performance of blends, Mixing rules, Low-temperature performance, Solid-Liquid equilibrium, Modeling, Predictive UNIQUAC.

Abstract: In recent years, biodiesel has received a notable attention due its ability to replace fossil fuels. It is considered an environmental friendly due their vast advantages. This biofuel is obtained from renewable resources, so it is considered biodegradable, CO_2-neutral, non-toxic and significantly reduces the greenhouse gas emissions.

It is composed by a mixture of mono alkyl esters obtained from vegetable oil, such as, soybean oil, jatropha oil, rapeseed oil, palm oil, sunflower oil or from other sources like animal fat (beef tallow, lard), waste cooking oil and grasses. The most common process for its production is by a transesterification reaction, where the vegetable oil reacts with a short chain alcohol in presence of a catalyst.

Due to its properties very similar to diesel fuel, they are mutually miscible and so can be mixed in any proportion in order to improve its qualities. The knowledge of its thermophysical properties like density and viscosity, which are affected by temperature, is very import for automotive industries.

However, biodiesel present some disadvantages like higher viscosity, density, cloud and pour point compared with diesel fuel.

Its behaviour at low-temperature limiting its application in cold climate and these behaviour is influenced by raw materials and the alcohol used in production process. The biodiesel obtained from oils with a major level in saturated fatty acids esters induce a worse behaviour at low temperatures, since they are solid compounds at lower temperatures.

In this work, binary and ternary blends of biodiesel of soybean, rapeseed and palm, and diesel fuel were prepared and its dynamic viscosities and densities were measured in function of temperature. Mixing rules are used for predicting the densities and viscosities from pure compounds.

The low temperature behaviour of three biodiesel was studied. The liquid and solid phase compositions and solid fraction at temperatures below the cloud point were analyzed. A thermodynamic model was applied to describe these multiphase systems and other similar systems. Two versions of the predictive UNIQUAC model along with an approach that assuming complete immiscibility of the compounds in the solid phase are evaluated against the experimental phase equilibrium data measured.

List of Contents

List of Tables

List of Figures

Nomenclature

List of Symbols

ΔT	Boiling temperature of solution, K
m	Molality, mol.Kg^{-1}
k_b	Ebullioscopic constant
x	Molar fraction of the component
G	Interaction parameter
W	Massic fraction of the component
E_r	Maximum error, %
c	Fraction entrapped liquid
ΔH	Molar enthalpy, KJ.mol^{-1}
ΔC_p	Heat capacity, KJ.K^{-1}
g	Energy Gibbs, KJ.mol^{-1}
R	Gas Constant, Pa.m^3.mol^{-1}.K^{-1}
T	Temperature, K
N	Mixture component reference
q	Molecular shape
r	Molecular size
Z	Coordination number
A	Correlation parameter
B	Correlation parameter
IR	Refractive index
n	Number of molecules, mol
m_i	Mass of compound, g
M	Molecular weight, g.mol^{-1}

Greek letters

η	Viscosity of the component, mPa.s
ρ	Density of the component, g.cm^{-3}

φ	Property in study
γ	Activity coefficient of the component
ϕ	Molecular volume fractions
θ	Surface fractions
λ	Interaction energies
α	Interaction parameter

Subscripts

i , j	Pure components indexes
mix	Mixture
EXP	Experimental value
$\mathrm{Pr}ed$	Predictive value
E	Excess property
fus	Fusion
vap	Vaporization
sub	Sublimation
cy	Cyclohexane component
$Diesel$	Diesel component

Superscripts

P	Precipitated phase
S	Solid phase
L	Liquid phase
BD	Biodiesel

Abbreviations

GC	Gas chromatography
DSC	Differential Scanning Calorimetry
CP	Cloud Point, K

1. Introduction

1.1 Motivation and Objectives

The transport sector is today almost completely dependent of fossil fuels, particularly petroleum-based fuels such as gasoline, diesel fuel and liquefied petroleum gas (LPG). Due to the limited reserves of these fuels it is necessary to find out alternative fuels based on renewable resources, such as biodiesel. In recent years, biodiesel has gained importance because of its ability to replace diesel fuel. It is technically feasible, economically competitive and environmentally acceptable. This biofuel can be used neat or blended with diesel fuel in any proportion without requiring modifications in the motor.[1-2]

The density and viscosity of biodiesel and their temperature dependence are two important properties. Viscosity is important for modeling combustion processes such as, injection systems, pumps and injectors. The density is important for optimization and simulation in numerous chemical engineering unit operations. These properties can be estimated using blending or mixing rules as function of composition based on pure component values. [2-3]

The winter use of biodiesels is the another important problem, since biodiesels have higher cloud points than petroleum based diesel. It is thus necessary to study their behavior at low temperatures.[4-6]

The present work is motivated by the importance of knowing the thermophysical properties and behavior t low temperatures behavior of biodiesels for their application.

This work will carry the synthesis of three biodiesels (from Soybean(S), Palm(P) and Rapeseed(R) by a transesterification reaction with methanol and its composition characterization by GC-FID. In order to analyze its physical properties, density and dynamic viscosity of its blends (S+R, S+P, SRP) and blends with diesel are measured at temperatures ranging from (283.15 to 363.15) K and then compared with the data obtained by mixing rules. The low temperature behavior of the biodiesels is study through the solid-liquid equilibrium. Experimental data obtained are compared with two versions of the predictive UNIQUAC model along with a model assuming complete immiscibility of the compounds on the solid phase.

1.2 Introduction

The limited reserves of fossil fuels, the constant oscillation of the petroleum prices and the increasing environmental concerns have led to a search for fuels from renewable resources, such as biodiesel and bioethanol.[7-10]

Bioethanol can be produced by the transformation of bio resources such as crops (like sugar cane or corn) or lignocellulosic biomass, but requires the conditioning or pretreatment of the feedstocks for fermenting organisms to convert them into ethanol. Then, it is necessary to separate and purify the ethanol from the fermentation broth (solution of water and ethanol). Distillation is the technique commonly used for this separation, but in order to reduce the energetic costs other processes have been developed, such as adsorption, liquid-liquid extraction, pervaporation, gas stripping and stream stripping.[11-13] Ethanol is employed in the transport sector as an additive for gasoline and in last few years, due the environmental issues and the continuous crises in crude oil prices, ethanol became a viable and realistic alternative fuel.[11]

Biodiesel is an alternative to diesel fuel. Chemically is a blend of mono-alkyl esters (generally methyl or ethyl esters) of long-chain fatty acids, produced from vegetable oils (sunflower oil, castor oil, soybeans oil, rapeseed oil, peanut oil, cottonseed oil, jatropha oil and others), animal fats (beef tallow, lard) and fish oil or even from waste cooking oil and greases [6, 9, 14]. These mixtures are constituted mainly by triglycerides with various levels of free fatty acids [5-6, 15]. The most common fatty acids found in vegetable oils are show in Table 1, where the *x* represents the number of carbons and *y* the number of unsaturations[15].

Table 1- Common fatty acids found in vegetable oils.[15]

Trivial name	IUPAC name	Structure $_{x:y}$ [a]	M_r	m.p. [ºC]	b.p. [ºC (kPa)]
Saturated					
Capric acid	Decanoic acid	10:0	172.3	32	239.7 (101.3)
Lauric acid	Dodecanoic acid	12:0	200.3	43	20.6 (101.3)
Myristic acid	Tetradecanoic acid	14:0	228.4	54	298.9 (101.3)
Palmitic acid	Hexadecanoic acid	16:0	256.4	62	309.0 (101.3)
Stearic acid	Octadecanoic	18:0	284.5	69	332.6 (68.3)
Arachidic acid	Eicosanoic acid	20:0	312.5	75	355.2 (68.3)
Behenic acid	Docosanoic acid	22:0	340.6	81	-
Monounsaturated					
Palmitoleic acid	9-hexadecenoic acid	16:1	254.4	0	-
Oleic acid	9-octodecenoic acid	18:1	282.5	13	334.7 (53.3)
Vaccenic acid	11-octadecenoic acid	18:1	282.5	7	-
Gadoleic acid	9-eicosenoic acid	20:1	310.5	25	-
Erucic acid	13-docosenoic acid	22:1	338.6	33	-
Polyunsaturated					
Linoleic acid	9,12-octadecadienoic acid	18:2	280.5	-9	230.0 (2.1)
A-linolenic acid	9,12,15-octadecatrienoic	18:3	278.4	-17	230.0 (2.3)
A-Linolenic acid	6,9,12-octodecatrienoic acid	18:3	278.4	-	-
Arachidonic acid	5,8,11,14-eicosatetraenoic acid	20:4	304.5	-50	-
EPA	5,8,11,14,17-eicosapentaenoic acid	20:5	302.4	-	-

[a] Number of carbon atoms (x) and number of unsaturated bonds

This alternative to conventional diesel has many advantages such as its biodegrability, non-toxicity, decrease in the energy dependency from fossil resources and contribution to the reduction in global warming through its use in the transport sector. [5, 8, 16-17]. The Figure 1 shows the comparison between biodiesel and diesel fuel emissions. It is visible a reduction in emissions with B100, except for the nitrogen oxide (NO_x). The oxygen present in alkaly chain of the biodiesel is an important factor for NO_x formation. During the combustion the hydrocarbons reacting with oxygen causing an increase in local temperatures and the formation of NO_x.[18]

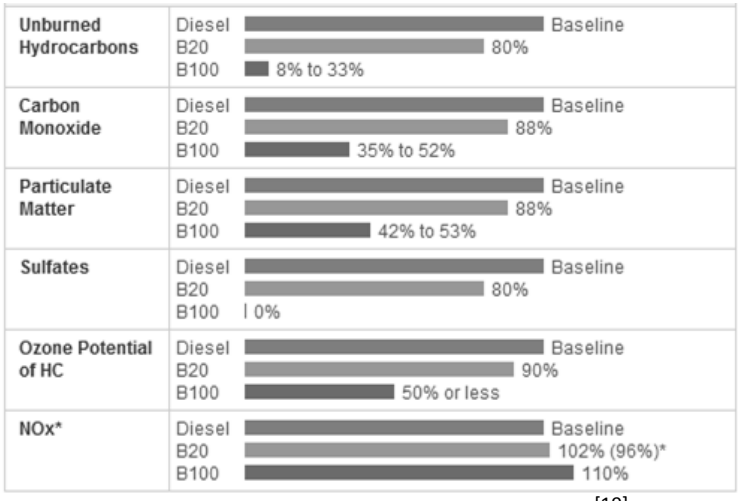

Figure 1- Comparison between biodiesel and diesel fuel emissions.[19]

In order to meet the targets of Kyoto Protocol, signed in January 2008, the European Union proposed the use of 5.75% of biodiesel into transportation sector by 2010 and 10% until 2020 [8, 15, 20]. Portugal as an ambitious mark and is currently using 7% of biodiesel on its commercial diesel fuel.[21]

There are various methods to produce biodiesel such as pyrolysis, microemulsion, cracking and transesterification [15, 22-23]. The last one is the most common in industrial biodiesel production. The transesterification process occurs through the action of a homogeneous catalyst (alkali or acid), a heterogeneous catalyst (e.g. immobilized enzyme) or with supercritical alcohol [14, 24].

Typically, biodiesel production has three principal processing sections: a transesterification section (1), a biodiesel purification step (2) and a glycerol recovery section (3).[25]

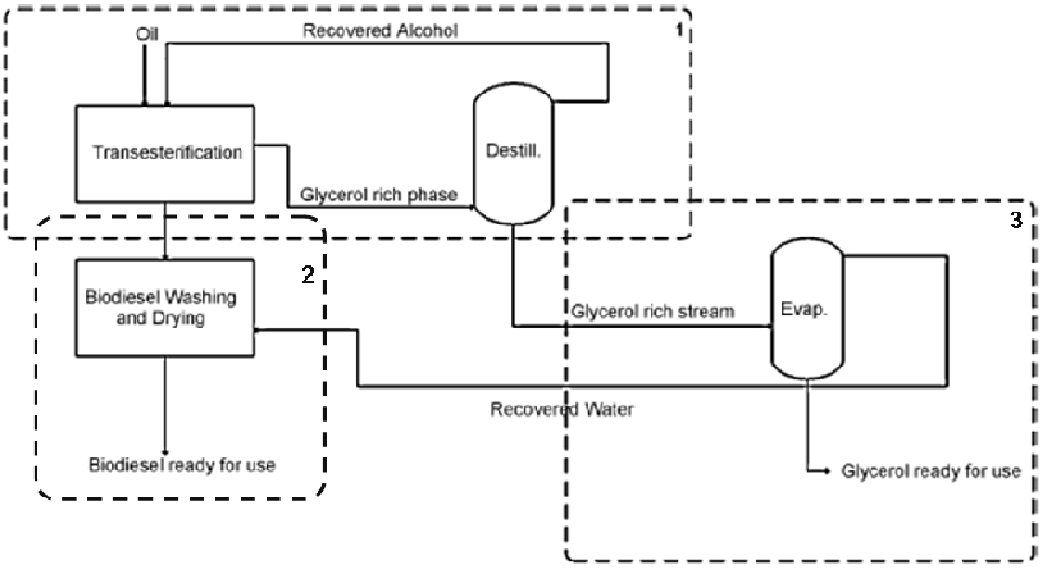

Figure 2-Simplified flowsheet for biodiesel production.[25]

The transesterification is a homogeneous reaction where the triglycerides react with a short-chain alcohol catalyzed by bases such KOH or NaOH, to produce two liquid phases: one of them rich in fatty alkyl esters (biodiesel) and the other in glycerol (secondary product) (Figure 2)[6, 25-28]. The unreacted alcohol is distributed between these two liquid phases. Methanol is the alcohol mostly used in this kind of reaction, due of its low cost and availability. It reacts promptly with triglycerides in presence of alkalis (Figure 3). Others alcohols can also be used, such as ethanol, butanol and propanol. [15, 25]

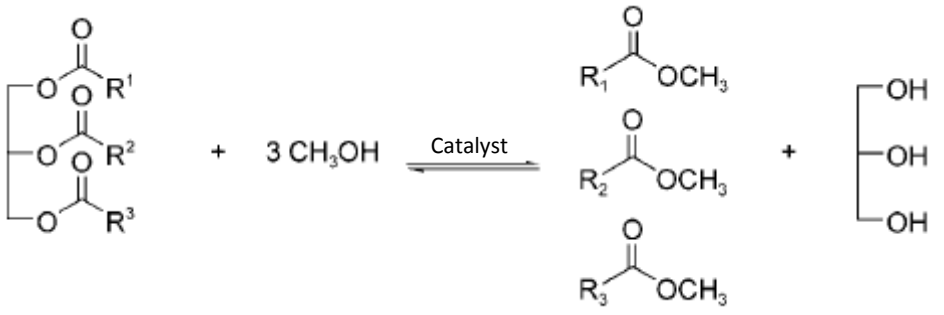

Figure 3-Transesterification reaction between triglyceride and methanol.[15]

The molar ratio of the alcohol-oil that should be used varies from 1:1 to 6:1. Nevertheless, to displace the reaction towards obtain the desired products is preferred a molar ratio 6:1 [27, 29]. The reaction rate is reasonably high even at 60ºC, but depending on the type of catalyst different temperatures will give different degrees of conversion and for that reason the temperature should be varies from 25ºC at 120ºC [27, 30]. Sodium hydroxide is less expensive and produces a high conversation and is often used in large-scale processing [14]. The concentration used of this base is the range of 0.5-1% by weight and yield a 94-99% conversion rate of most vegetable oils into esters [14, 27].

This process is more efficient (high conversion levels of triglycerides to their corresponding fatty acid alkyl esters in short reaction times), less corrosive to industrial equipment and much faster than a reaction using acid catalyst and thus the preferred in industrial practice [14, 30].

Alkaline transesterification have also many disadvantages, such as difficult recovery of glycerol, the requirement to remove the catalyst from the products, wastewater treatment, the necessity to use the oils without free fatty acids and the concentration of the water that interferes with the reaction [14, 23, 28, 31]. To prevent the soap formation, the amount of free fatty acids presents in oils should be lower than 0.5 wt% and the water concentration should be limited to 0.1 wt% or less. The soap formation not only consumes the alkali catalyst, but also can cause de formation of emulsions, which decrease yields and create difficulties in downstream recovery and purification of the biodiesel. [14-15, 27-29] These limitations mean that waste oils cannot be

processed by alkali catalysis without pretreatment to remove free fatty acids and water [32].

The acid catalysis is not much used industrially. It uses an acid, usually a sulfuric acid, phosphoric acid, hydrochloric acid or organosulfonic acid as catalyst. Although this type of catalysis gives a high yield in esters, the reaction is very slow and the acids are corrosive. [15, 27-30] Acid catalysis can be used with vegetable oil containing high free fatty acids without soap formation, but need higher temperatures (around 55ºC at 80ºC) and higher molar ratio of the alcohol-oil (up to 30:1) [29, 32].

The glycerol recovery section is an important step of the process because according to the European Standard EN 14214 and United States of America norm ASTM D6751, the maximum free glycerol amount admissible in biodiesel is 0.02% (wt%). Glycerol can be removed of biodiesel by washing with water, because the high affinity between glycerol and water. [25, 33] The glycerol rich stream is composed by glycerol and other chemical substances such as water, organic and inorganic salts, a small amount of esters and alcohol and a residue of glycerides. The exact composition depends on the transesterification reaction and the separation conditions of biodiesel production, but the glycerol concentration is usually between 30 to 60 wt%.[34] The alcohol present in the glycerol rich phase can be recovered by distillation and resent into the transesterification section. The water content present in the glycerol rich stream, from the bottom of the distillation column is then evaporated achieves the specifications necessary for commercial glycerol (Figure 2). The commercialization of the glycerol reduces biodiesel production costs in 22% - 36%. [25]

Recently, enzymatic transesterification has been suggested as an alternative for biodiesel production [7, 24, 35]. Enzymes are biocatalysts with a substrate specificity, functional group specificity and stereo specificity [36]. They offer several advantages, since they require less energy consumption, are reusable, the presence of free fatty acids increases yield, works even in the presence of water without soap formation, are more compatible with variations in the quality of the raw materials, have low impact in the environment (less noxious products and waste), the catalyst can be easily recovered and the purification of biodiesel is simpler [7, 16, 27-29, 37]. This process also has disadvantages

such as the high cost of enzyme, low reaction rate and the loss of activity [16]. The loss of activity may be caused by many factors, *e.g.* leakage of enzyme from supports when they are attached during immobilization, inhibition by the substrate, thermal inactivation and the loss of their spatial conformation leading to changes in the active site [22].

Lipases (EC 3.1.1.3, *triacylglycerol acylhydrolases*) are the most popular enzymes for synthesis of the biodiesel. The most studied enzyme is the Novozym 435, a commercial lipase B from *Candida Antarctica* immobilized in acrylic resin [28, 31].

Lipase is an enzyme that is responsible for the hydrolysis of triglycerides into diglycerides, monoglycerides, glycerol and fatty acids, so they are classified by hidrolases. It catalyzes also the transesterification/ esterification of lipids into biodiesel.[38-39]

Industrially, the application of enzymes for biodiesel production is economically unattractive, due to the high cost of their production, purification and stabilization [16, 32, 40].

Biodiesel can be distributed in pure form (B100) or blends (Bx) where the x represents the amount of biodiesel in the blend. This biofuel is much simpler than conventional diesels, being made just by a handful of fatty acid esters. The knowledge of the basic properties of biodiesel-diesel blends is required for the design and optimization of biodiesel production plants.[2, 41] Density data are import for many chemical engineering unit operations, for storage tanks and for process piping. This property of an ethyl/methyl ester biodiesel is influenced by its molecular weight, free fatty acid content, water content and temperature. Viscosity is the other thermophysical property important for engine performance, because modern fuel-injection systems are sensitive to viscosity changes and high viscosity leads to poor atomization of the fuel, incomplete combustion, choking of the fuel injectors and ring carbonization.[3, 41-43] In Table 2 are presented requirements and methods for test the quality of biodiesel according to standard norm EN 14214:2003.

Table 2- EN 14214:2003 requirements and test methods for biodiesels.[44]

PROPERTY	UNIT	MINIMUM	MAXIMUM	TEST METHOD
ESTER CONTENT	% (M/M)	96.5		PREN 14103
DENSITY @ 15°C	KG/M3	860	900	EN ISO 3675 EN ISO 12185
VISCOSITY @ 40°C	MM2	3.5	5.0	EN ISO 310
FLASH POINT	°C	ABOVE 101		ISO / CD 3679
SULFUR CONTENT	MG/KG		10	
CARBON RESIDUE (10% BOTTOMS)	% (M/M)		0.3	EN ISO 10370
CETANE NUMBER		51.0		EN ISO 5165
SULPHATED ASH CONTENT	% (M/M)		0.02	ISO 3987
WATER CONTENT	MG/KG		500	EN ISO 12937
TOTAL CONTAMINATION	MG/KG		24	EN 12662
COPPER STRIP CORROSION (3HR @ 50°C)	RATING	CLASS 1	CLASS 1	EN ISO 2160
OXIDATION STABILITY, 110°C	HOURS	6		PR EN 14112
ACID VALUE	MG KOH/G		0.5	PR EN 14104
IODINE VALUE			120	PR EN 14111
LINOLENIC ACID METHYL ESTER	% (M/M)		12	PR EN 14103
POLYUNSATURATED (>= 4 DOUBLE BONDS) METHYL ESTERS	% (M/M)		1	
METHANOL CONTENT	% (M/M)		0.2	PR EN 14110
MONOGLYCERIDE CONTENT	% (M/M)		0.8	PR EN 14105
DIGLYCERIDE CONTENT	% (M/M)		0.2	PR EN 14105
TRIGLYCERIDE CONTENT	% (M/M)		0.2	PR EN 14105
FREE GYLCEROL	% (M/M)		0.02	PR EN 14105 PR EN 14106
TOTAL GYLCEROL	% (M/M)		0.25	PR EN 14105
ALKALINE METALS (NA + K)	MG/KG		5	PR EN 14108 PR EN 14109
PHOSPHORUS CONTENT	MG/KG		10	PR EN 14107

Not only the properties but the behavior and performance of a biodiesel also depends on the raw materials used on the production process. The oils and alcohol used in the reaction affect its cold flow performance. Oils with large concentration of saturated fatty acids ester, such as palm oil, even though less vulnerable to oxidation and displaying better lubricating and combustion properties, at low temperatures present a higher tendency to form solid deposits. Saturated fatty acids have higher melting points and crystallize at higher temperatures than unsaturated fatty acids. This can be explained by the unsaturated fatty acids often having a *cis* isomer, making difficult the packing of molecules in a crystal, hindering the development of an organized solid, unlike saturated fatty acids, which due to its linear chain, can easily interact and crystallize. Because of the limitations of the biodiesel performance at low temperatures, there are quality standards

defined and the most important are the cloud point (CP; EN 23015 and ASTM D-2500), the pour point (PP; ASTM D-97 and ASTM D-5949), the cold filter plugging point (CFPP; EN 116, IP-309, and ASTM D-6371), and the low temperature filterability test (LTFT; ASTM D-4539).[5-6, 20] These properties are important for the biodiesel production and commercialization, allowing their safe use in countries with cold climates.[5-6]

Table 3-Fatty acid composition in common vegetable oils and fats.[45]

Fat or oil	Fatty acid (%)														Saturated (%)	Unsaturated (%)
	6:0	8:0	10:0	12:0	14:0	16:0	16:1	18:0	18:1	18:2	18:3	20:0	22:0	22:1		
Canola						3.9	0.2	1.9	64.1	18.7	9.2	0.6	0.2		6.6	92.2
Coconut	0.5	8.0	6.4	48.5	17.6	8.4		2.5	6.5	1.5		0.1			92.0	8.0
Corn						12.2	0.1	2.2	27.5	57.0	0.9	0.1			14.5	85.5
Olive						13.7	1.2	2.5	71.1	10.0	0.6	0.9			17.1	82.9
Palm				0.3	1.1	45.1	0.1	4.7	38.5	9.4	0.3	0.2			51.4	48.3
Rapeseed					0.1	2.8	0.2	1.3	21.8	14.6	7.3	0.7	0.4	34.8	5.3	78.7
Safflower					0.1	6.5		2.4	13.1	77.7		0.2			9.2	90.8
Soybean					0.1	10.9	0.1	4.2	25.0	52.7	6.2	0.3	0.1		15.6	84.0
Sunflower				0.5	0.2	6.8	0.1	4.7	18.6	68.2	0.5	0.4			12.6	87.4
Beef tallow			0.1	0.1	3.3	25.5	3.4	21.6	38.7	2.2	0.6	0.1			50.7	44.9

The CP is the temperature at which crystallization of the heavier fatty acid esters starts when the fluid is cooled and the solution becomes cloudy. With the continuous decrease of temperatures, the crystal particles grow and agglomerate, reducing the capacity of the liquid to flow through porous media by plugging the fuel filters, the temperature at which the filters blocks calls the CFPP. Eventually, the crystal net formed in bulk liquid gels the fluid completely and the PP is attained. The presence of solid crystals in this biofuel affects its viscosity, volatility, flowability and filterability. [5-6]

Generally, biodiesel has a higher CP, PP and CFPP than conventional diesel. The high values of these properties can be a problem for the use of biodiesel. In attempt for solve these problems, efforts have been made to create additives that improve cold properties of biodiesel.[5-6] Additives are usually polymeric molecules that are based on operational co-crystallization with the molecules of saturated esters to change the size and growth rate of its crystals. Those molecules bind to the ester chain crystals at different points, preventing the aggregation among themselves as they are trapped in the binding sites. Although there is retention of crystals in the filter engine, the layer uptake is significantly more permeable to the passage of fuel compared to the non-use of additives. [46]

Alternatively, the manipulation of the composition of biodiesel can improve their properties at low temperatures. One way is maintaining a mixture of esters at temperatures between the CP and PP, precipitating the saturated esters in the form of suspension into bulk liquid. The filtrated biodiesel treated is poorer in saturated esters, improving it performance in cold weather, this process is called *winterization*. [46]

The cold properties of the biodiesel can be predicted by knowledge of its composition [5-6]. There are many techniques that can be used to characterize these compositions. The most widely used are gas chromatography (GC) and high performance liquid chromatography (HPLC). GC is a separation technique, extremely reliable, which allows the separation of fatty acids present in oils and esters. [47]

The CP is the only propriety that can be defined thermodynamically and modeled. The others proprieties (PP, CFPP and LTFT) are linear functions of the CP, thus can be determined from the CP. It is possible to develop a thermodynamic model to predict the CP value from the knowledge of the fluid composition. Such model would be very important to evaluate the cold flow properties and design formulations of oil blends in biodiesel production. [5-6]

2. Experimental Procedure

2.1 Synthesis of biodiesels produced from Soybean, Rapeseed and Palm oils

2.1.1 Materials

Palm and rapeseed oils were obtained from Sovena, Portugal. Soybean oil was obtained from Bunge Iberica, Portugal. Potassium hydroxide pure was used as a catalyst for transesterification and obtained from Pronalab. Methanol with purities of 99.9% was obtained from Lab-Scan. Sodium sulphate anhydrous was supplied by JMGSantos.

2.1.2 Biodiesels Synthesis

The biodiesels of palm, rapeseed and soybean were produced in the laboratory by a transesterification reaction. The molar ratio of oil/alcohol was 1:5 with 0.5% sodium hydroxide by weight as the catalyst. The reaction temperature and time were 45ºC and 45 minutes, respectively (**Appendix A**). The biodiesels were stored in the dark, hermetically sealed in glass bottles, kept at the room temperature to prevent contamination and alteration of their properties.

2.2 Characterization of Biodiesels

2.2.1 GC

The chromatograph used was a Varian 3800CP (Figure 4) equipped with a split injector at 250ºC and a FID detector at 220ºC. The injection was made with a split ratio of 1:20, using a Hamilton syringe and an amount of sample of 0.5 µL, previously diluted (10 µL of biodiesel for 1000 µL of the dichloromethane). The column used was a Select™ Biodiesel FAME with a length of the 30 m, internal diameter of the 0.25 mm and a film thickness of the 0.25 µm, coater with a film of polyethylene glycol. The carrier gas was helium with a flow rate of 2 mL/min. It was used a temperature program of 4ºC/min from 120ºC at 250ºC.

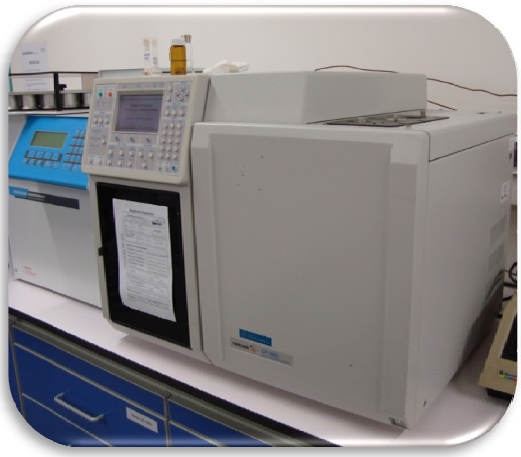

Figure 4-Varian 3800 CP GC-FID

2.2.2 Densities and Viscosities

2.2.2.1 Binary and Ternary Blends of Biodiesel

2.2.2.1.1 Preparations of blends and measurement

The binary and ternary blends of biodiesels were prepared using the same proportion of the various biodiesels. Densities and dynamic viscosities of the three biodiesels and their blends here studied were measured using an automated SVM 3000 Anton Paar rotational Stabinger viscometer-densimeter at atmospheric pressure (Figure 5). These two properties were measured for biodiesels of soybean and rapeseed at temperatures from (283.15 to 363.15) K and biodiesel of palm, binaries and ternary blends were measured at temperatures from 293.15 to 363.15 K. Every measurement was done three times to obtain average values and standard deviations for each temperature (**Appendix B**).

Figure 5- Automated SVM 3000 Anton Paar rotational Stabinger viscometer-densimeter.

2.2.2.2 Binary Blends of Biodiesel and Diesel fuel

2.2.2.2.1 Materials

Biodiesels of soybean, rapeseed and palm used here were synthesized in section 2.1 by a transesterification reaction and diesel fuel was obtained from Galp, Portugal.

2.2.2.2.2 Preparations of blends and measurement

Biodiesel blends were prepared in the following proportions: 20% (B20), 40% (B40), 60% (B60) and 80% (B60) (wt%). Densities and dynamic viscosities of the binary blends of biodiesels with diesel fuel were measured according with the procedure described above. Every measuring was done three times to obtain average values and standard deviation for each temperature (**Appendix C**).

2.2.2.2.3 Determination of molecular weight of Diesel fuel

The determination of diesel fuel molecular weight was calculated using colligative property, the boiling point elevation, that depend on the number of molecules in a given volume of solvent. The boiling point of the solution is achieved when the equilibrium between liquid and gas phases are established and this corresponds to the number of gas

molecules that entering in systems is equal to the number of vapour molecules leaving the system. Then, an addition of solute destabilizes the system, so for compensate this and re-attain the equilibrium, boiling point increases.[48]

This phenomenon can be related by expression,

$$\Delta T = m \times k_b \quad (1)$$

where ΔT is the boiling temperature change of the solution, m is the molality of the solution and k_b is the ebullioscopic constant of solvent. The solvent used in this work is the cyclohexane (99.9% purity obtained from Aldrich) and the value of its ebulliscopic constant is 2.79 ºC.Kg.mol^{-1}.[49]

The equipment used in this experimental procedure was an ebulliometer (Figure 6) that is composed by a boiling still with a port for liquid sampling/injection and a condenser.

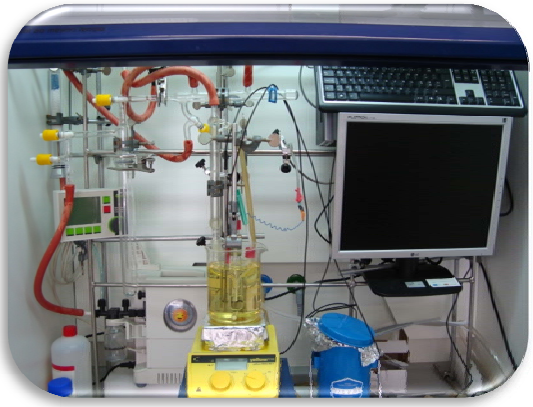

Figure 6- Ebulliometer.

The temperature control was made using a thermostatic bath. For measure the boiling point of pure cyclohexane, an amount of this solvent was introduced into the boiling still and heated to its boiling point while mixing with a magnetic stirrer. The temperature was measured using a calibrated Pt100 temperature sensor with an uncertainty of 0.05 K. When the boiling point was reached, a sample of this solution was collected and the refractive index measured. Subsequently amounts of diesel fuel were introduced into the ebulliometer to change the mixture composition and the procedure was repeated.

Refractive index measurements were used for analyzing the composition of these samples, using an Abbe type refractometer (Figure 7), with an uncertainty of $1x10^{-4}$.

Figure 7-Abbe refractometer.

To perform the calibration curve of the equipment, samples were prepared with different amounts of cyclohexane and diesel, and the refractive indexes were read at controlled temperature of 30ºC (**Appendix C**).

The refractive index shows a linear trend with the fraction weigh of diesel. Through this correlation it is possible to obtain the composition of the samples removed from the ebulliometer and then, calculate the molecular weight of the diesel.

2.2.2.3 Mixing Rules

The basic properties of blends as a function of pure properties of components can be estimated using mixing rules.

The viscosity of liquid mixtures can be predicted for mixing rule originally proposed by Arrhenius and described by Grunberg and Nissan[50],

$$\ln \eta_{mix} = \sum_{i}^{N} x_i \ln \eta_i + \sum_{i}^{N} \sum_{j}^{N} x_i x_j G_{ij} \qquad (2)$$

where η_{mix} is the liquid mixture viscosity, η_i is the viscosity of the component i, x_i and x_j are the molar fractions of the component i and j, respectively, G_{ij} is the interaction parameter and n is the number of pure components in the mixture.

When the components of a mixture have a similar chemical structure, such as, biodiesel and diesel fuel (both liquids are non-polar, completely miscible and where are blended their volumes are practically additive), it is considered that they do not interact with each other and consequently the interaction parameter G_{ij} is neglected.[2, 51-52] The final mixing rule is show in Equation 3,

$$\ln \eta_{mix} = \sum_{i}^{N} x_i \ln \eta_i \tag{3}$$

The density of mixture can be obtained using Kay´s mixing rule,

$$\rho_{mix} = \sum_{i}^{N} W_i \rho_i \tag{4}$$

where ρ_{mix} is the density of mixture, W_i is the massic fraction of the component i and ρ_i is the density of the component i.[2]

The percentage of error between experimental data and predictive values obtained by mixing rules are calculated by

$$Er(\%) = \left(\frac{\varphi_{Exp} - \varphi_{\Pr ed}}{\varphi_{\Pr ed}} \right) \times 100 \tag{5}$$

where φ is the property to be predicted and the subscripts are Exp for experimental and $\Pr ed$ for predicted.

2.3 Biodiesels Behaviour at low temperatures

2.3.1 DSC

Differential scanning calorimetry (DSC) is a thermal analysis technique for measuring the heat flow energy associated with transitions in materials as a function of temperature, such as melting and crystallization. In the case of endothermic and exothermic processes, this technique provides qualitative and quantitative information about physical and chemical properties.[53]

DSC analysis was performed using a Perkin Elmer Diamond DSC equipment, where the samples were tightly sealed in aluminium pans. The quantity of biodiesel used was previously weighed on a microanalytical balance and ranged from 5 to 15 mg. The sample and reference were heated simultaneously at a temperature rate of 2ºC/min from -70ºC to 30 ºC. The temperature was constantly monitored and the power required to keep the two cells at the same temperature was registered.

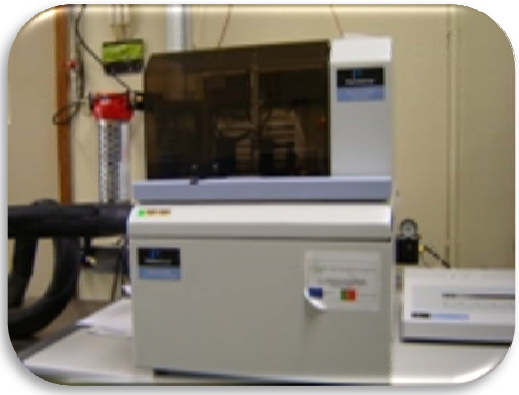

Figure 8-Perkin Elmer Diamond DSC.

2.3.2 Experimental Procedure

The behaviour of the three biodiesels synthesized (soybean, rapeseed and palm) at low temperatures was studied using a methodology previously developed to measure solid-liquid phase equilibrium in hydrocarbon fluids[54-55] and widely used to study both

synthetic mixtures and diesels[54, 56-59]. It consists of separating the liquid phase from the precipitate by filtration at a controlled temperature and analyzing booth phases by gas chromatography. The phase separation was achieved using a UniPrep™ syringeless filters from Whatman of 5 mL capacity with filters of 0.2 µm porosity. The biodiesel was introduced on a thermostatic bath, where the samples were equilibrating for 24h before separation. When the separation was completed, the two phases (liquid, L, and precipitate, P) recovered were analyzed using a chromatographic procedure identical to that used previously for the study of compositions of biodiesels synthesized.

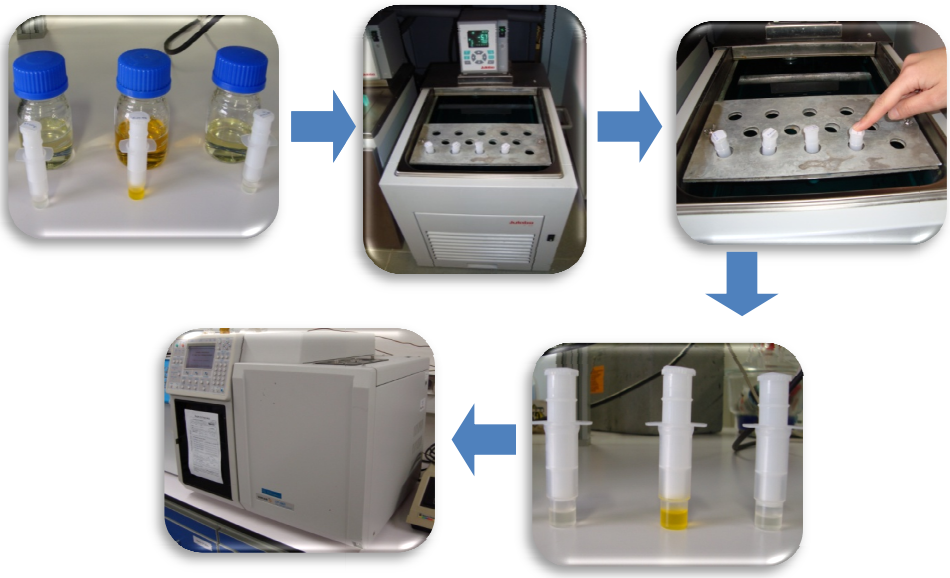

Figure 9-Scheme of experimental procedure.

The liquid and solid phase composition and fractions was estimated by mass balances from the results of these analysis according to a procedure proposed previously[54-55] and detailed below. No multiple measurements were carried out of each point; therefore, a correct value of repeatability of experimental data cannot be assigned. On the basis of others works[54-59], where the results for the points were duplicated, the estimated reproducibility is 1% on the liquid phase composition, 5% on the solid-phase composition and 5-10% on the solid fraction.

The precipitate (P) recovered is composed by the solid phase (S) and important quantities of liquid (L) that remain entrapped in the crystals after the filtration. It is thus impossible to assess directly the composition of the solid phase after the filtration. Only

the composition of the liquid phase (L) and precipitate (P) can be determined directly. Because the unsaturated fatty acid esters have melting points much lower than the corresponding saturated fatty acid esters, they will not crystallize at the temperatures used on this study, and thus, the portion of liquid entrapped in the crystals of the precipitate can be determined from the quantity of unsaturated fatty esters present in liquid phase, known from chromatography. It is possible to calculated the fraction entrapped liquid, c, as

$$c = \frac{W_{C18:1}^{P} + W_{C18:2}^{P} + W_{C18:3}^{P}}{W_{C18:1}^{L} + W_{C18:2}^{L} + W_{C18:3}^{L}} \tag{6}$$

where W is the mass fraction of the compounds obtained from the chromatographic analysis and P and L stand for the precipitate and liquid fractions. Using the value of this fraction, c, it is possible to estimate the composition of the various compounds i present in the solid phase, S, as

$$W_i^S = \frac{W_i^P - cW_i^L}{1-c} \tag{7}$$

The fraction of the initial biodiesel sample that crystallized, X^s, can be obtained from a mass balance to any of the compounds present but is ideally estimated from the concentration of any of the unsaturated fatty acid esters on both the original biodiesel, BD, and the concentration in the liquid phase, L, under the conditions studied as

$$X^s = \frac{W_i^L - W_i^{BD}}{W_i^L} \tag{8}$$

This experimental methodology allows an easy measurement of the composition of the liquid, W^L, and solid, W^S, phases as well as the fraction of crystallized material, X^S, as a function of the temperature.

2.3.3 Thermodynamic model

The precipitation of solids in biodiesel at low temperatures was described here using an approach previously proposed for alkane mixtures[54, 60-74] and also applied to fatty acids[75] and fatty acids methyl and ethyl esters[5, 76] with success.

The solid-liquid equilibrium can be described by an equation relating the composition of component i in the solid and liquid phases with their non-ideality an the thermophysical properties of the pure component[77]

$$\ln \frac{x_i^s \gamma_i^s}{x_i^l \gamma_i^l} = \frac{\Delta_{fus} H_i}{R T_{fus,i}} \left(\frac{T_{fus,i}}{T} - 1 \right) - \frac{\Delta_{fus} C_{p,i} \left(T_{fus,i} \right)}{R} \left(1 - \frac{T_{fus,i}}{T} + \ln \frac{T_{fus,i}}{T} \right) \quad (9)$$

where γ_i is the activity coefficient of the compound, x_i is its mole faction, $\Delta_{fus} H(T_{fus})$ is the molar enthalpy of fusion of the pure solute at the melting temperature T_{fus}, and $\Delta_{fus} C_{p,i} \left(T_{fus,i} \right)$ is the molar heat capacity change upon fusion at fusion temperature T_{fus}. The heat capacity change upon fusion is usually regarded as being independent of the temperature, and the term in parentheses multiplied by $\Delta_{fus} C_{p,m}$ is often considered as being small, because the opposite signs inside the parentheses lead to near cancellation.[78] This term was thus neglected on the calculations. The thermophysical properties of the crystallizing saturated fatty acids esters used were obtained from correlations developed in a previous work[76] and are reported in Table 4.

Table 4-Thermophysical properties of saturated fatty acid methyl esters.

Fatty acid methyl esters	T_{fus} / K	$\Delta_{fus} H / kJ.mol^{-1}$	$\Delta_{vap} H / kJ.mol^{-1}$
C16:0	302.59	56.85	96.58
C18:0	311.45	64.84	105.92

Since the major compounds of a biodiesel are fatty acid esters of similar size and nature, the liquid phase may be treated as an ideal solution. Using Equation 6, along with a multiphase flash algorithm, the composition and amount the liquid phase may be

treated as an ideal solution of the phases in equilibrium can be calculated if a model for the non-ideality of the solid phases is available. Because of its simplicity and robustness, the algorithm of resolution of the Raschford-Rice equations proposed by Leibovici and Neoschil[79] was used in the calculations.

The solid phase non-ideality is described by the most recent version of the UNIQUAC model.[63] The UNIQUAC model can be written as

$$\frac{g^E}{RT} = \sum_{i=1}^{N} x_i \ln\left(\frac{\Phi_i}{x_i}\right) + \frac{Z}{2}\sum_{i=1}^{N} q_i x_i \ln\frac{\theta_i}{\Phi_i} - \sum_{i=1}^{N} x_i q_i \ln\left[\sum_{j=1}^{N} \theta_j \exp\left(-\frac{\lambda_{ij}-\lambda_{ii}}{q_i RT}\right)\right] \qquad (10)$$

with

$$\Phi_i = \frac{x_i r_i}{\sum_j x_j r_j} \quad \text{and} \quad \theta_i = \frac{x_i q_i}{\sum_j x_j q_j} \qquad (11)$$

On this version of predictive UNIQUAC, the structural parameters, r_i and q_i, are obtained from UNIFAC parameter table.[80]

The predictive local composition concept[54, 60-63] allows for the estimation of the interaction energies, λ_{ij}, used by these models without fitting to experimental data. The pair interaction energies between two identical molecules are estimated from the heat of sublimation of the pure component

$$\lambda_{ii} = -\frac{2}{Z}\left(\Delta_{sub}H_i - RT\right) \qquad (12)$$

where Z is the coordination number with value of 10 as in the original UNIQUAC model.[63, 81] The heats of sublimation are calculated at the melting temperature of the pure component as

$$\Delta_{sub}H = \Delta_{vap}H + \Delta_{fus}H \qquad (13)$$

The pair interaction energy between two non-identical molecules is given by

$$\lambda_{ij} = \lambda_{ji} = \lambda_{jj}\left(1+\alpha_{ij}\right) \qquad (14)$$

where j is the ester with shorter chain of the pair ij. The interaction parameter α_{ij} allows for the tuning of the non-ideality of the solid solution. In this work, three approaches to the solid phase non-ideality will be evaluated: assuming $\alpha_{ij} = 0$ (UNIQUAC), as was previously performed for alkanes[54, 60-74] using $\alpha_{ij} = -0.05$ (UNIQUAC – 0.05), a value similar to that used on the description of the phase diagrams of fatty acids[75] and fatty acid esters,[4] and finally, assuming that there is no solid solution formation and each compound crystallizes as a pure crystal (no solution). This last situation corresponds to an infinite value of the solid phase activity coefficient that within the framework of predictive UNIQUAC can be achieved with a value of α_{ij} larger than -0.25.

The solid-liquid equilibrium model used in this work is thus a purely predictive model that uses only pure component properties for the calculation of the phase equilibrium. The three versions evaluated here will be used to predict the low-temperature behaviour of the three biodiesels studied in this work and also to the experimental data of the three biodiesel measured in a precious work[82] (**Appendix D**).

3. Discussion and Results

3.1 Synthesis of biodiesels

The composition of four major components of the biodiesel here in study was represented in Table 5.

Table 5-Compositions (wt %) of the biodiesels studied.

	BD Soybean	BD Rapeseed	BD Palm
C16:0	10.91	5.77	41.37
C18:0	3.20	1.37	3.65
C18:1	22.39	64.36	44.56
C18:2	55.50	21.63	10.18
C18:3	8.00	6.87	0.24

3.2 Densities and Viscosities

3.2.1 Binary and Ternary Blends of Biodiesel

The results indicated in Figure 10 show the variations of viscosity for pure biodiesels and its blends with temperature. In the case of pure biodiesels the viscosity, for a fixed temperature, decreases in the following order, palm, soybean and rapeseed biodiesel. This fact can be explained by the increase of unstaurations that leads to a smaller contact area available for interaction, inducing thus, an increase in entropy of liquid phase caused by the double bonds and consequent decrease in viscosity. Viscosity-temperature curves for pure biodiesels and several blends exhibit a similar trend for temperature variation and small differences in the viscosities of the pure biodiesels.

The variation of dynamic viscosity with temperature has been commonly represented by Arrhenius equation,

$$\ln \eta = A + \frac{B}{T} \tag{15}$$

where A and B are correlation parameters. These constants and the regression coefficient (R^2) for each regression curve are presented in Table 6. The minimum regression coefficient (R^2) for viscosity is 0.9978, which means that equation represents a good fit to the relationship between viscosity and temperature for biodiesels tested.

Table 6-Regression parameters for viscosity.

	A	B	R^2
B100 Palm	-5.5555	2274.2	0.9985
B100 Rapeseed	-5.4192	2184.7	0.9979
B100 Soybean	-5.4561	2236.6	0.9983
B50 Soybean+B50 Rapeseed	-5.3639	2188.2	0.9978
B50 Soybean+B50 Palm	-5.3402	2199.0	0.9985
B50 Rapeseed+B50 Palm	-5.3842	2196.3	0.9985
Ternary Mixture	-5.3349	2187.0	0.9986

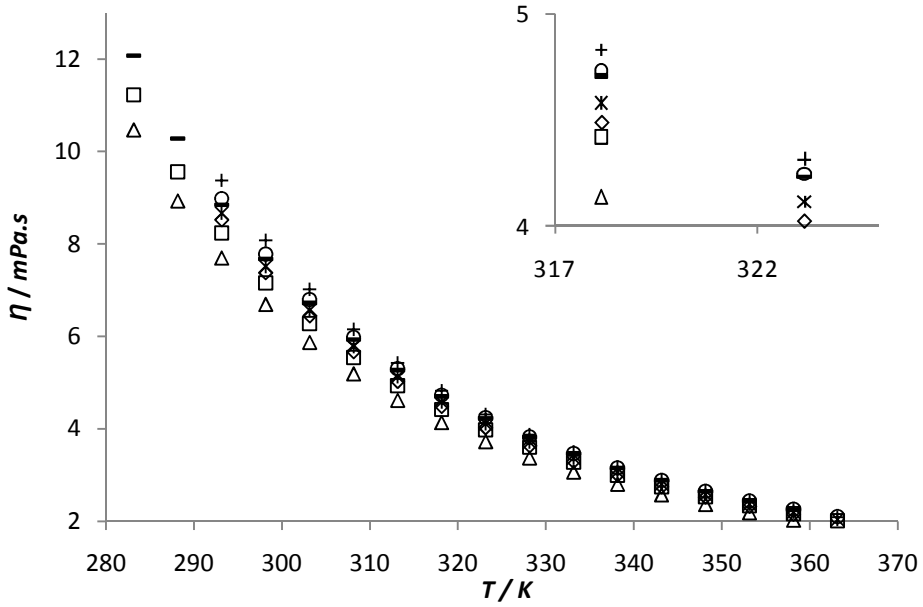

Figure 10-The effect of temperature in dynamic viscosities of pure biodiesels and its blends: + B100 Palm, ○ B50 Soybean+B50 Palm, – B100 Soybean, ✳ Ternary Mixture, ◇ B50 Rapeseed+B50 Palm, □ B50 Soybean+B50 Rapeseed, △ B100 Rapeseed.

Viscosities of the binary and ternary blends of biodiesels as a function of temperature are compared with the predictive results to verify the mixing rule (Equation 3). Comparisons are shown in Figure 11.

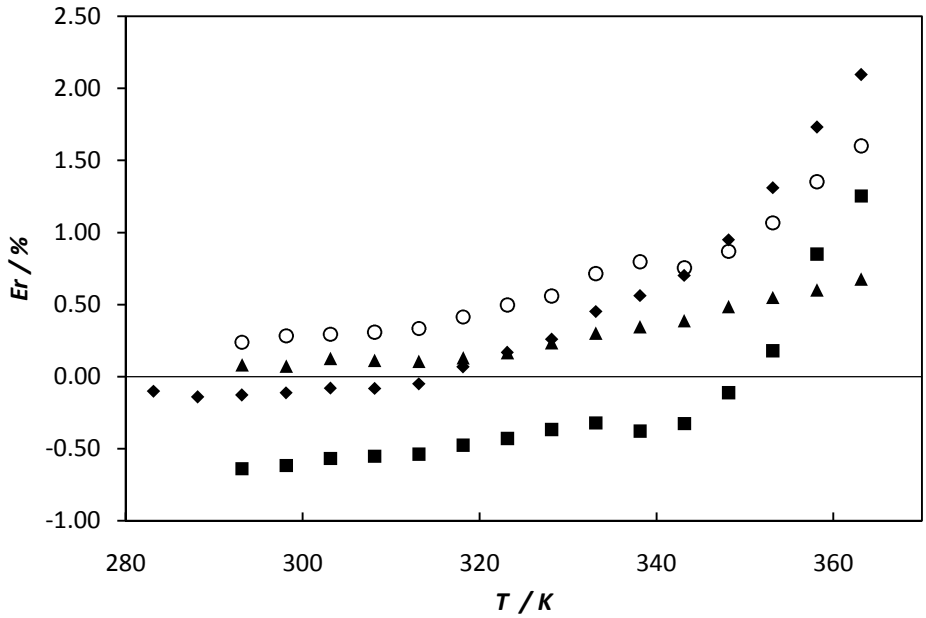

Figure 11-Relative deviations between experimental and predictive data for viscosity as a function of temperature: ○ Ternary mixture, ▲ B50 Rapeseed+B50 Palm, ◆ B50 Soybean+B50 Rapeseed, ■ B50 Soybean+B50 Palm. Zero line is this work´s experimental data.

The maximum relative error is less than 2.1%, indicating that mixing rule is suitable for predicting the basic properties of these biodiesels and its blends as a function of temperature.

In **Figure 12**Figure 12, all results show a linear decrease in density with the temperature. For the case of pure biodiesels the density, at fixed temperature, decreases in the following order, soybean, rapeseed and palm biodiesel. The decrease of the level of unsaturations causes a decrease in density. Experimental data were correlated by linear regressions, Equation 16, and the results are presented in Table 7.

$$\rho = A + B\,(T) \tag{16}$$

Table 7-Linear regressions parameters for blends densities.

	A	B	R^2
B100 Palm	1.0943	-0.0007	0.999988
B100 Rapeseed	1.0979	-0.0007	0.999995
B100 Soybean	1.1021	-0.0007	0.999987
B50 Soybean+B50 Rapeseed	1.1012	-0.0007	0.999988
B50 Soybean+B50 Palm	1.0992	-0.0007	0.999996
B50 Rapeseed+B50 Palm	1.0962	-0.0007	0.999994
Ternary Mixture	1.0982	-0.0007	0.999996

The regression coefficients (R^2) are always superior to 0.999987, indicating as expected, that linear regression accurately represents the relationship between density and temperature for the mixtures tested.

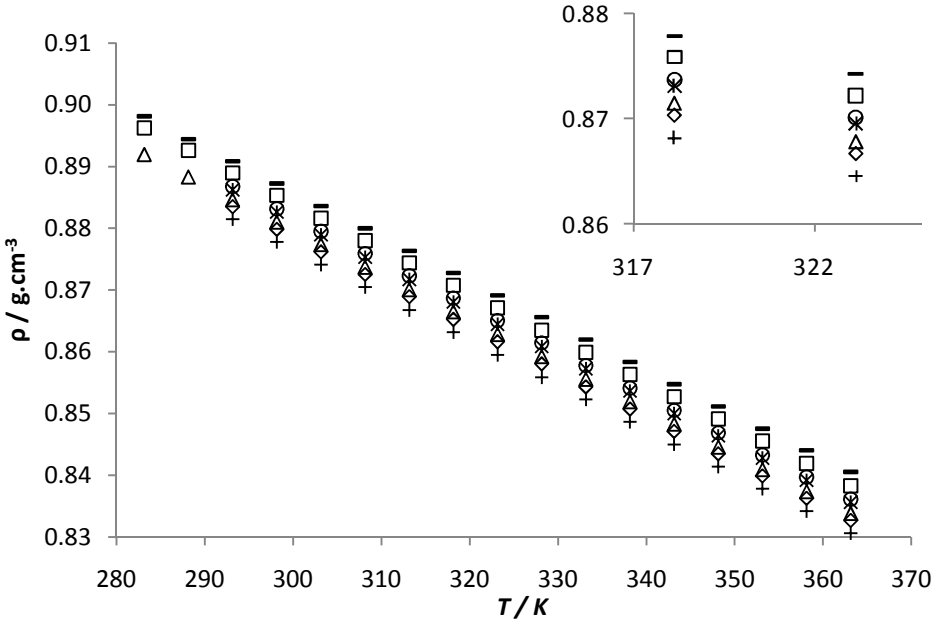

Figure 12-The effect of temperature in densities of pure biodiesels and their blends: – B100 Soybean, □ B50 Soybean+B50 Rapeseed, ○ B50 Soybean+B50 Palm, × Ternary Mixture, △ B100 Rapeseed, ◇ B50 Rapeseed+B50 Palm, + B100 Palm.

Experimental data are compared with predictive values obtained by Equation 5 for density. The results are shown in Figure 13.

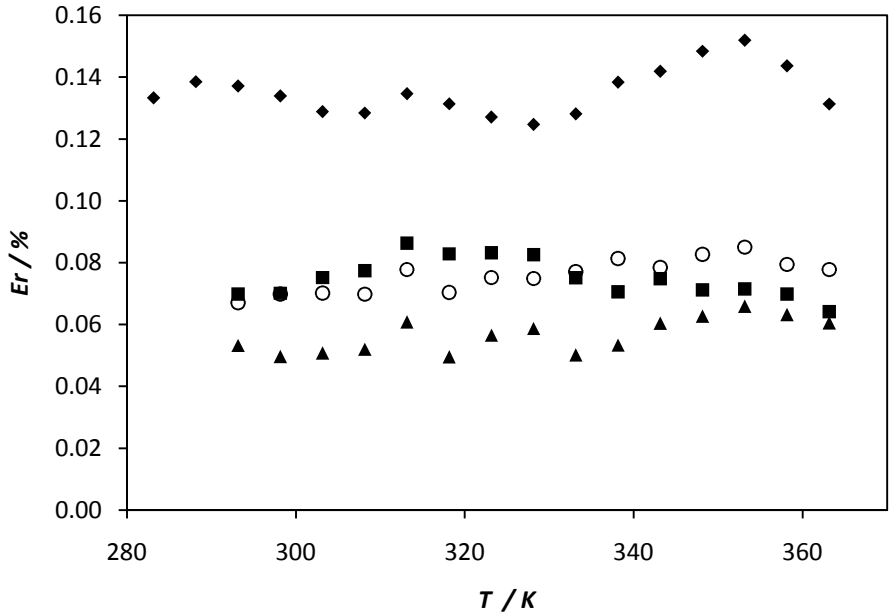

Figure 13- Relative deviations between experimental and predictive data for density as a function of temperature: ◆ B50 Soybean+B50 Rapeseed, ■ B50 Soybean+B50 Palm, ○ Ternary mixture, ▲ B50 Rapeseed+B50 Palm. Zero line is this work´s experimental data.

The maximum difference between experimental and predictive value is always less than 0.16%. These results demonstrated that model can be used for predict the density of the mixtures in study with good results.

3.2.2 Binary Blends of Biodiesel and Diesel fuel

Figure 14 shows the results of the calibration curve for system cyclohexane-diesel fuel. The calibration curve obtained,

$$IR = 0.0398 W_{Diesel} + 1.4198 \quad (17)$$

where IR is the refractive index and W_{Diesel} is the massic fraction of diesel fuel in mixture.

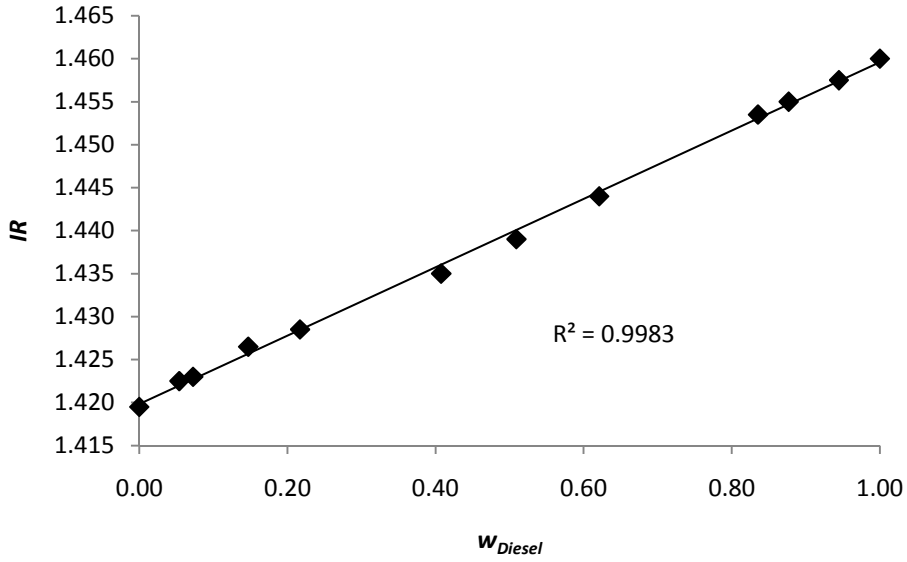

Figure 14-Calibration curve cyclohexane + Diesel fuel.

Replacing in Equation 1 the molality, m, by their definition is obtained the expression

$$\Delta T = k_b \times \frac{n_{Diesel}}{m_{Diesel} + m_{cy}} \times 1000 \tag{18}$$

where k_b is the ebulioscopic constant of cyclohexane, n_{Diesel} is the number of molecules presents in solution, m_{Diesel} is the mass of diesel fuel and m_{cy} is the mass of ciclohexane.

Manipulating Equation 18 and substituting n_{Diesel} by their definition,

$$\Delta T = \frac{1000 k_b}{M_{Diesel}} \times \frac{m_{Diesel}}{m_{Diesel} + m_{cy}} \tag{19}$$

where M_{Diesel} is the molar weight and m_{Diesel} is the mass of diesel fuel. The final equation obtained by manipulation of Equation 19 is

$$\Delta T = \frac{1000\, k_b}{M_{Diesel}} \times W_{Diesel} \quad (20)$$

where W_{Diesel} is the massic fraction of diesel fuel. Representing ΔT in function of W_{Diesel} (Figure 15), it is possible calculated the molecular weight by the slope of the Equation 21, because the slope is equal to ebullioscopic constant of cyclohexane, k_b, and molecular weight of diesel fuel, M_{Diesel}. The molecular weight obtained for the diesel fuel is 284.04 g.mol^{-1}.

$$\Delta T = 9.823\, W_{Diesel} \quad (21)$$

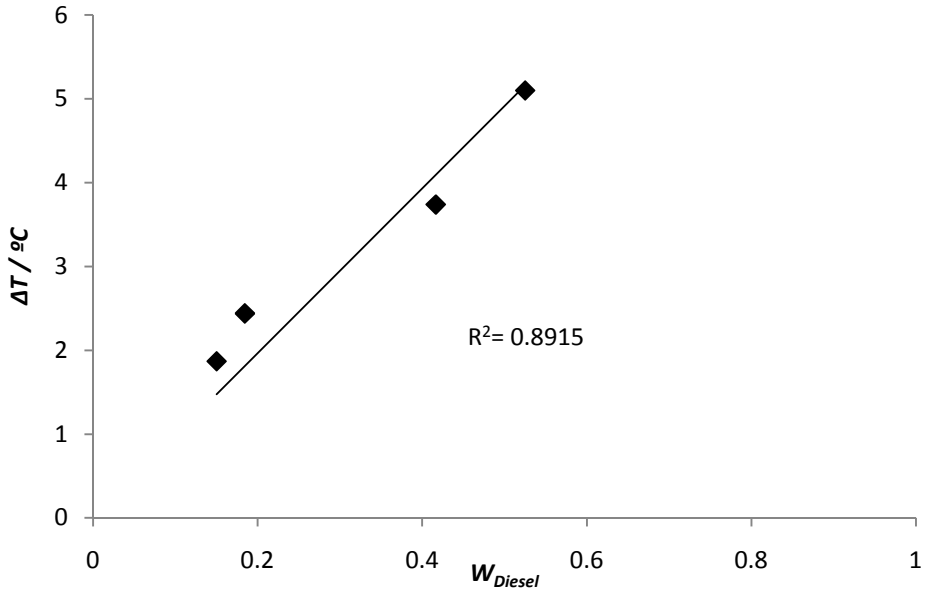

Figure 15-The effect of molality of diesel in temperature.

In Figure 16, Figure 17 and Figure 18, the results indicate that all viscosities of blends, diesel and biodiesel decreases with an increase of temperature. In the case of the binary blend of biodiesel-diesel fuel the viscosity increases in accordance with an increase in the blending ratio (B20 for B80), at temperature fixed. These results can be explained

by the fact of the differences in the chemical structure of biodiesel and diesel fuel. The first is a mixture of mono alkaly ester of saturated and unsaturated long chain fatty acids and the other is a mixture of paraffinic, naphthenic and aromatic hydrocarbons, hence the area for interact in the case of the molecules in pure diesel fuel are smaller than for molecules of pure biodiesel, so the viscosity increases with an increase of biodiesel in blend.

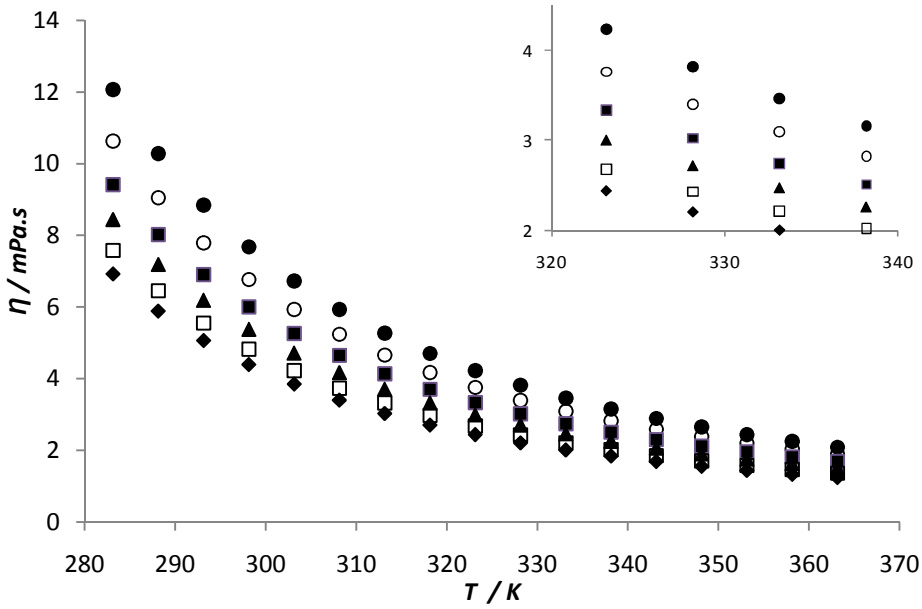

Figure 16-The effect of temperature in dynamic viscosities of soybean biodiesel, diesel fuel and their blends: ● B100, ○ B80, ■ B60, ▲ B40, □ B20, ◆ Diesel fuel 100.

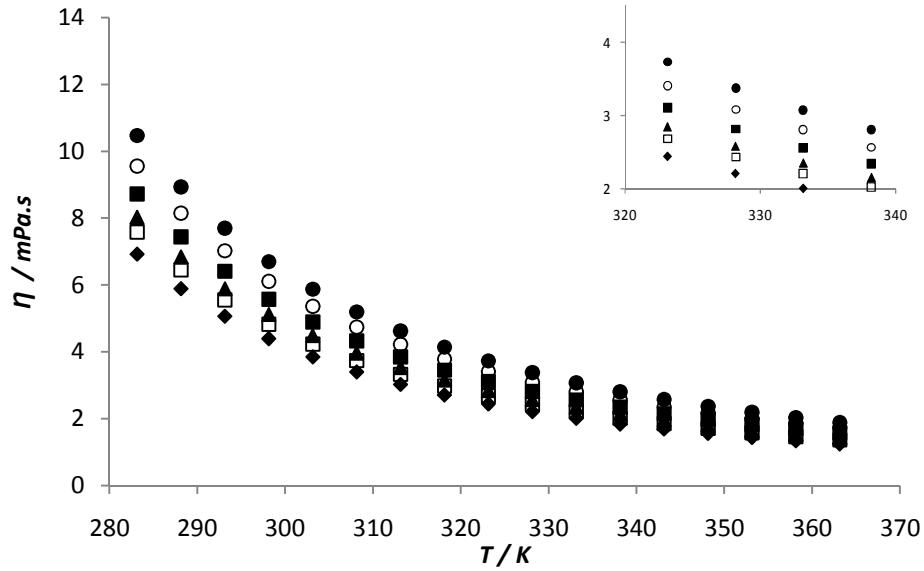

Figure 17-The effect of temperature in dynamic viscosities of rapeseed biodiesel, diesel fuel and their blends: ● B100, ○ B80, ■ B60, ▲ B40, □ B20, ◆ Diesel fuel 100.

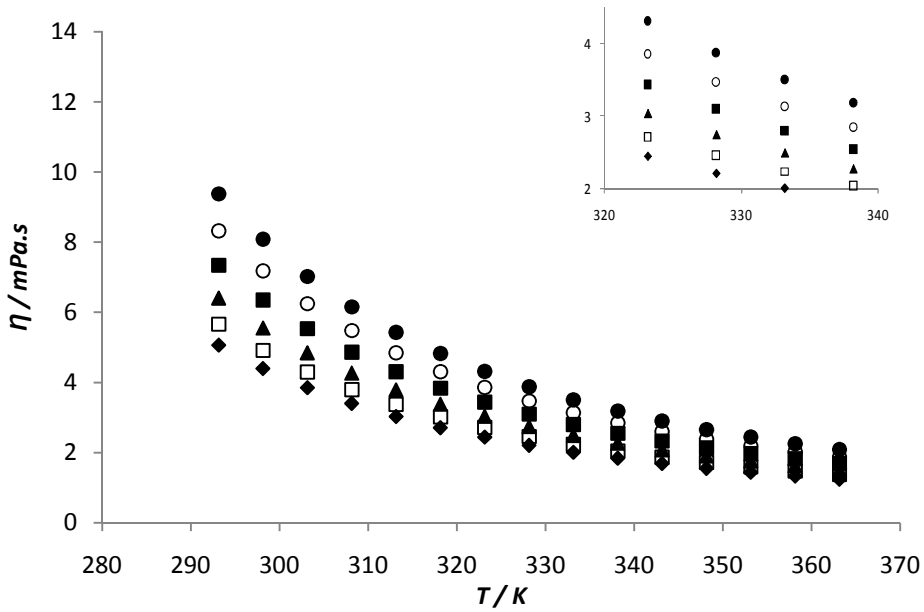

Figure 18-The effect of temperature in dynamic viscosities of palm biodiesel, diesel fuel and their blends: ● B100, ○ B80, ■ B60, ▲ B40, □ B20, ◆ Diesel fuel 100.

The predictive results obtained for viscosities of biodiesel-diesel blends by Equation 3 are compared with experimental data. The value maximum for predictive error is 5% (Figure 19). These results indicating that predictive model for viscosities are able to provide a good description of this property.

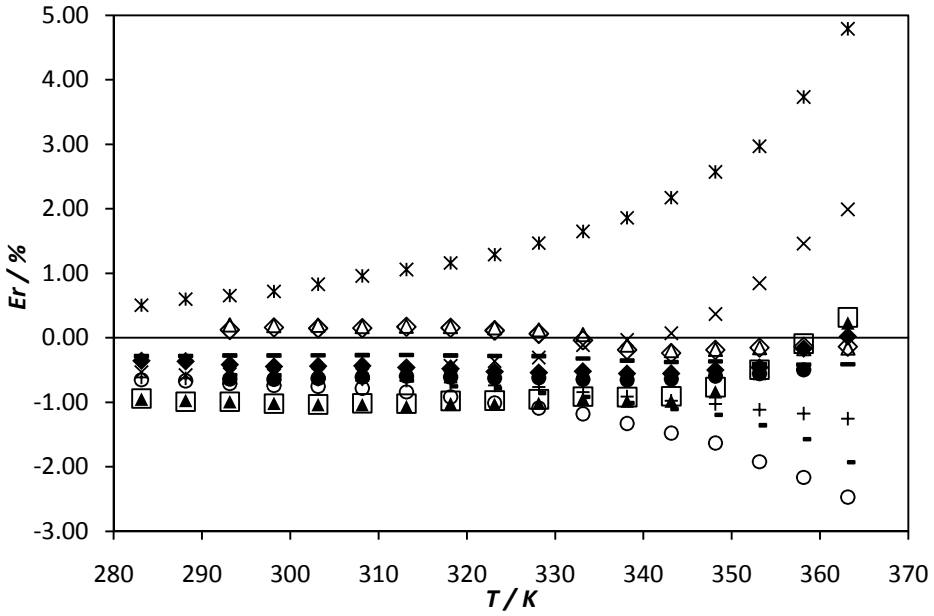

Figure 19- Relative deviations between experimental data and predictive for viscosity as a function of temperature: ✳ B20 Rapeseed, ◇ B60 Palm, △B80 Palm, × B80 Soybean, − B80 Rapeseed, ● B20 Palm, ◆ B20 Soybean, + B60 Rapeseed, ○ B40 Rapeseed, - B40 Palm, □ B40 Soybean, ▲ B60 Soybean. Zero line is this work´s experimental data.

Figure 20, Figure 21 and Figure 22 show the variations in density of biodiesels, diesel and their blends. The results demonstrate that density has temperature-dependence behavior linearly. At a fixed temperature, the density of all biodiesels has major than diesel fuel and in their blends the density increases with an increase in the blending ratio, due its chemical structure, the molecules of biodiesel have a lower molecular packing efficiency and that causes an increase in density. In addition, it can be seen a decrease in density with increasing temperature.

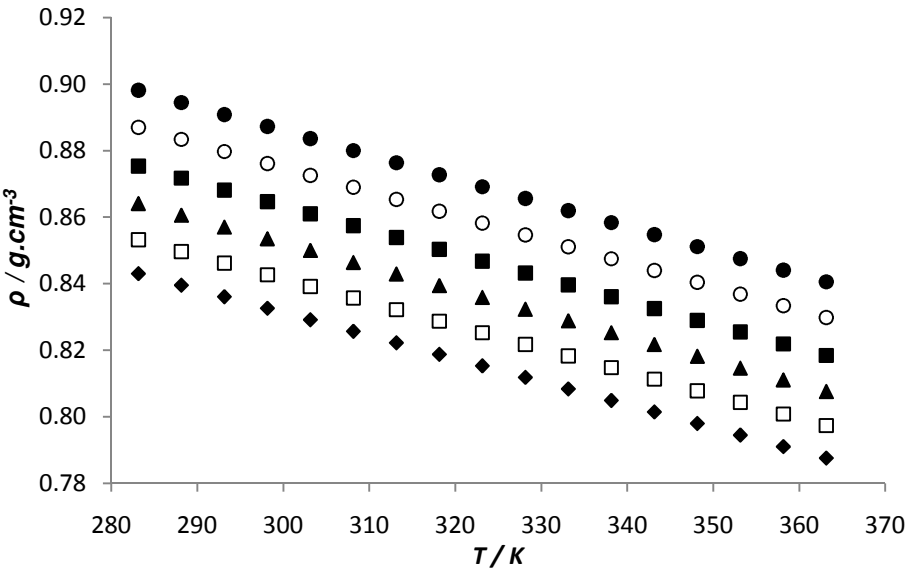

Figure 20-The effect of temperature in densities of soybean biodiesel, diesel fuel and their blends: ● B100, ○ B80, ■ B60, ▲ B40, □ B20, ◆ Diesel fuel 100.

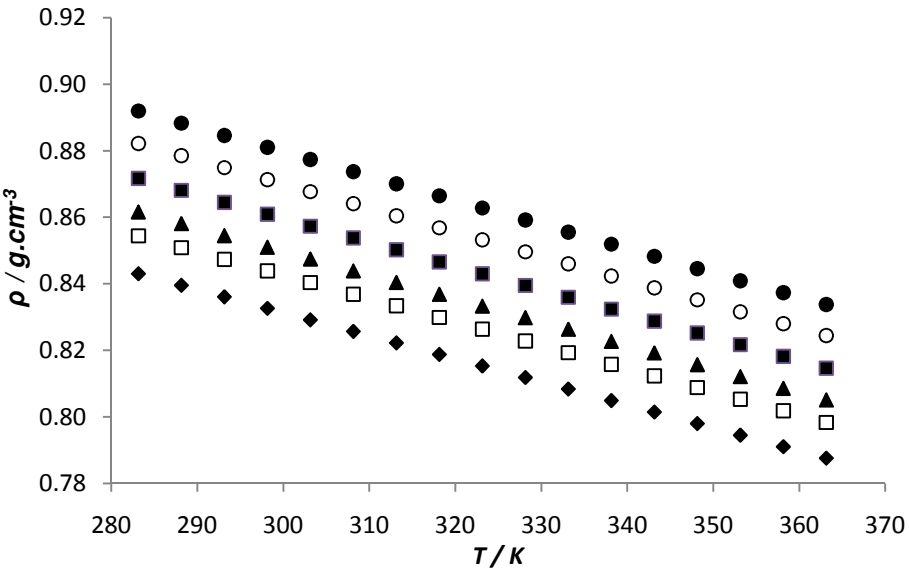

Figure 21-The effect of temperature in densities of rapeseed biodiesel, diesel fuel and their blends: ● B100, ○ B80, ■ B60, ▲ B40, □ B20, ◆ Diesel fuel 100.

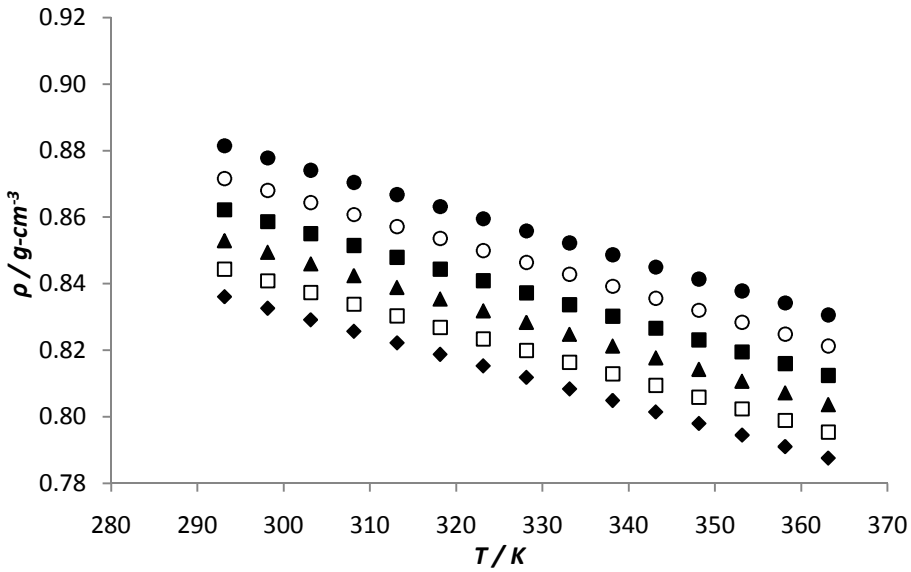

Figure 22-The effect of temperature in densities of palm biodiesel, diesel fuel and their blends: ● B100, ○ B80, ■ B60, ▲ B40, □ B20, ◆ Diesel fuel 100.

Experimental data are compared with predictive values obtained by Equation 4. The maximum predictive error calculated is 0.2% (Figure 23). These results demonstrated that model can be predicting the densities of blends in study.

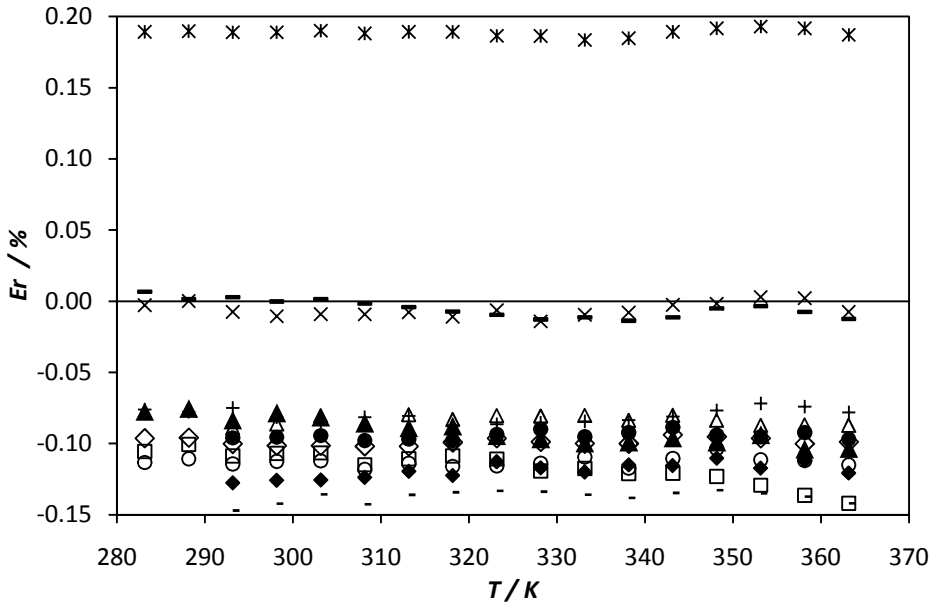

Figure 23- Relative deviations between experimental data and predictive for density as a function of temperature: ✳ B20 Rapeseed, - B80 Rapeseed, × B80 Soybean, + B60

Rapeseed, △B80 Palm, ▲ B60 Soybean, ● B20 Palm, ◇B20 Soybean, ⊓ B40 Soybean, ⊃ B40 Rapeseed, ◆ B60 Palm, - B40 Palm. Zero line is this work´s experimental data.

Experimental data for all blends biodiesel/biodiesel and biodiesel/diesel are compared with available data in literature. The results are shown in Figure 24.

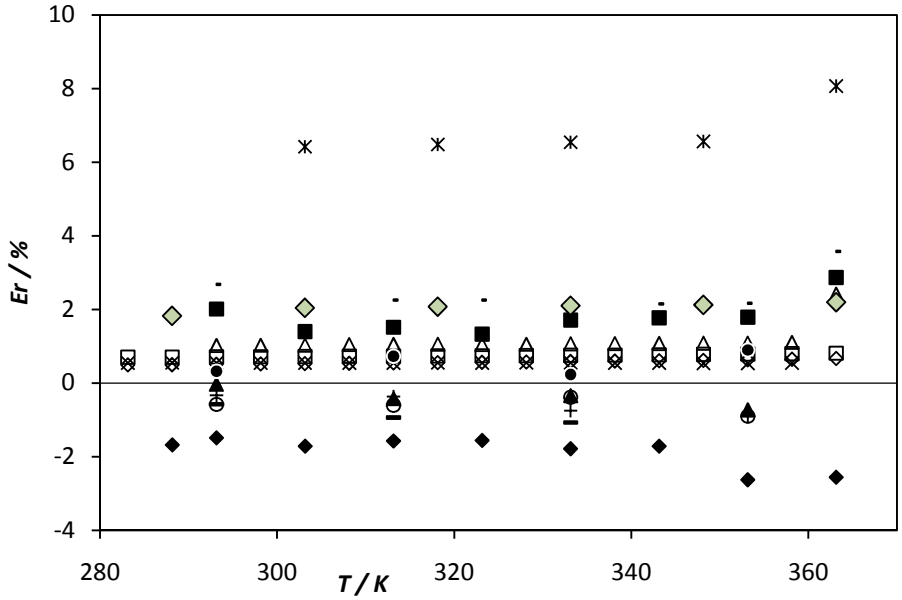

Figure 24- Relative deviations between experimental and literature data for density as a function of temperature: ◇ D100 (*Dzida et al)*, □ B20 Rapeseed+D80, △ B100 Palm *(Baroutian et al)*, × B100 Rapeseed, – B20 Soybean+D80, ⊃ B40 Soybean+D60, + B60 Soybean+D40, ▲ B80 Soybean+D20, ● B100 Soybean, ■ B100 Palm *(Benjumea et al),* - B20 Palm+D80, ◆ D100 *(Benjumea et al)*, ◈ D100 *(Baroutian et al)*, ⨯ B20 Palm+D80 *(Baroutian et al)*.[2, 41, 83-84]

The relative error obtained for comparison between experimental data and the literature, can be explained for several reasons, such as, the origin of the raw material for biodiesel production, the experimental conditions of measurements be different and the equipment used for measuring in this work providing a measure with more precision.

3.3 Biodiesels Behaviour at low temperatures

Figure 25, Figure 26 and Figure 27 show the thermograms obtained by DSC for biodiesel of soybean, rapeseed and palm. All thermograms demonstrated two fusion peaks. The first peak represents the fusion of the unsaturated methyl esters and the second the fusion of saturated methyl esters.

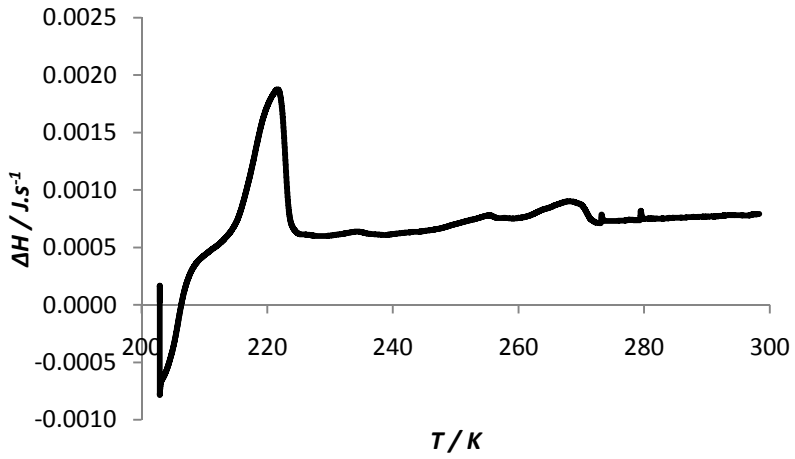

Figure 25-Thermogram for biodiesel of soybean

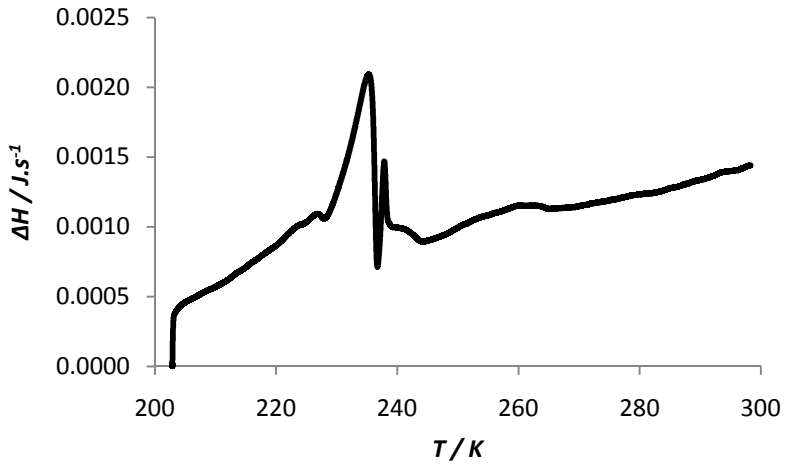

Figure 26-Thermogram for biodiesel of rapeseed.

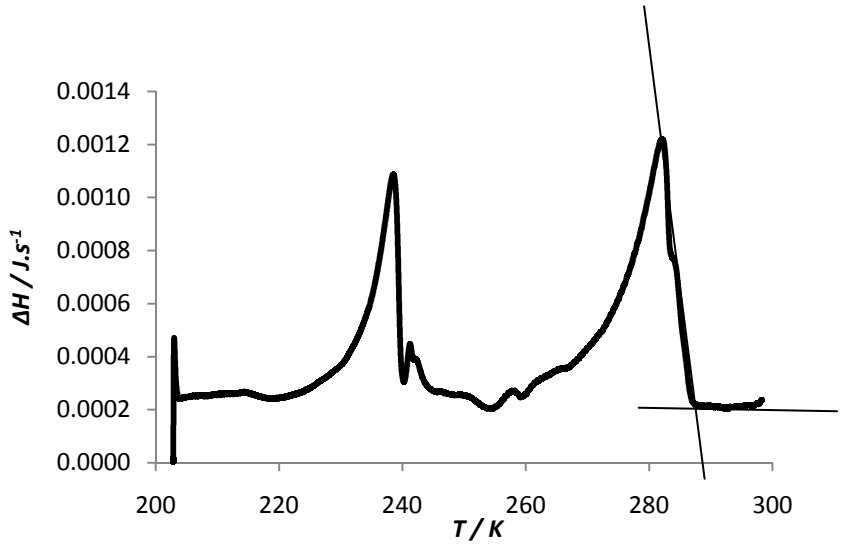

Figure 27-Thermogram for biodiesel of palm.

Tracing two tangent lines in the second peak is possible to determine the CP through its intersection (an example is demonstrated in Figure 27). The CP obtained for biodiesels in study is presented in Table 8.

Table 8-Values of CPs obtained by DSC for biodiesels.

	Biodiesel of soybean	Biodiesel of rapeseed	Biodiesel of palm
CP / K	270.9	263.5	286.7

The behaviour at low temperatures of biodiesel is evaluated here. The results obtained by thermodynamic models (UNIQUAC, UNIQUAC-0.05 and No Solution) are compared with experimental data for liquid-solid phase and solid fraction present in biodiesels. The Figures 30-47 show these comparisons and they are discussed below.

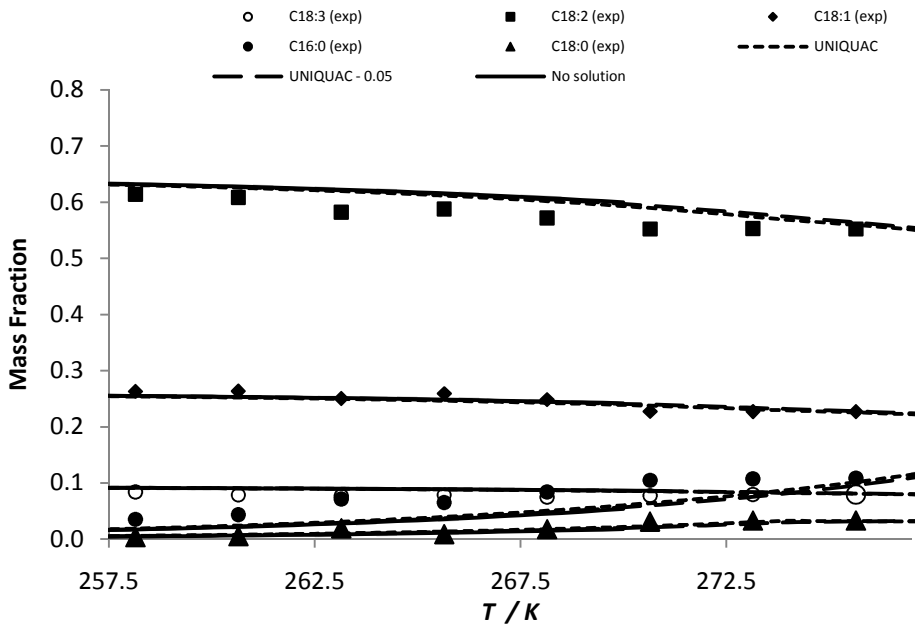

Figure 28-Liquid phase composition for biodiesel of soybean.

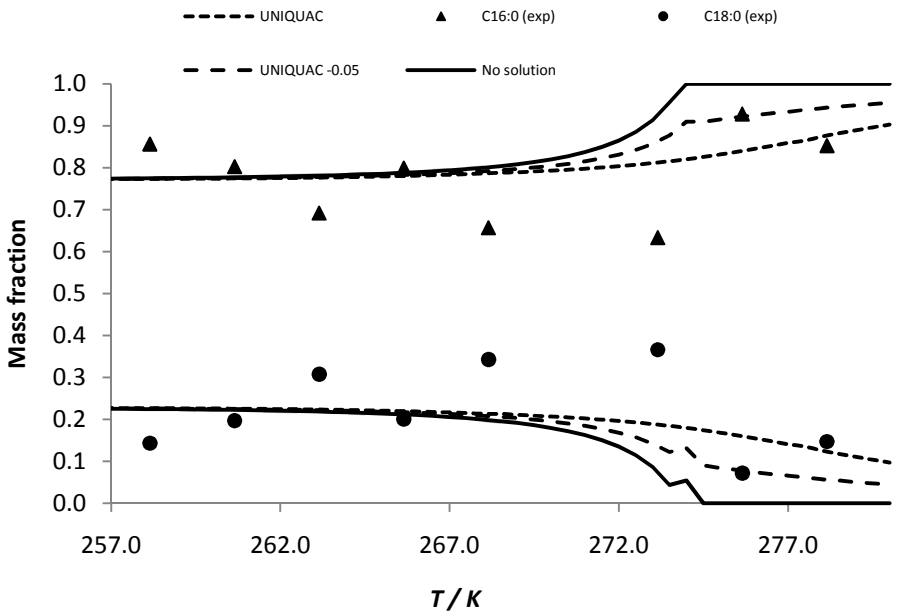

Figure 29-Solid phase composition for biodiesel of soybean.

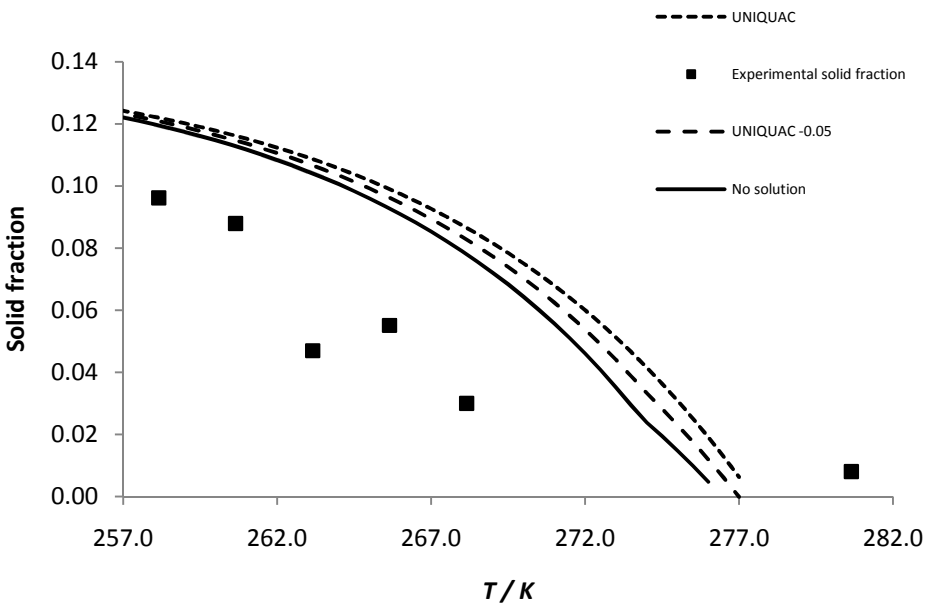

Figure 30-Dependence with temperature of the fraction of precipitated solid material for biodiesel of soybean.

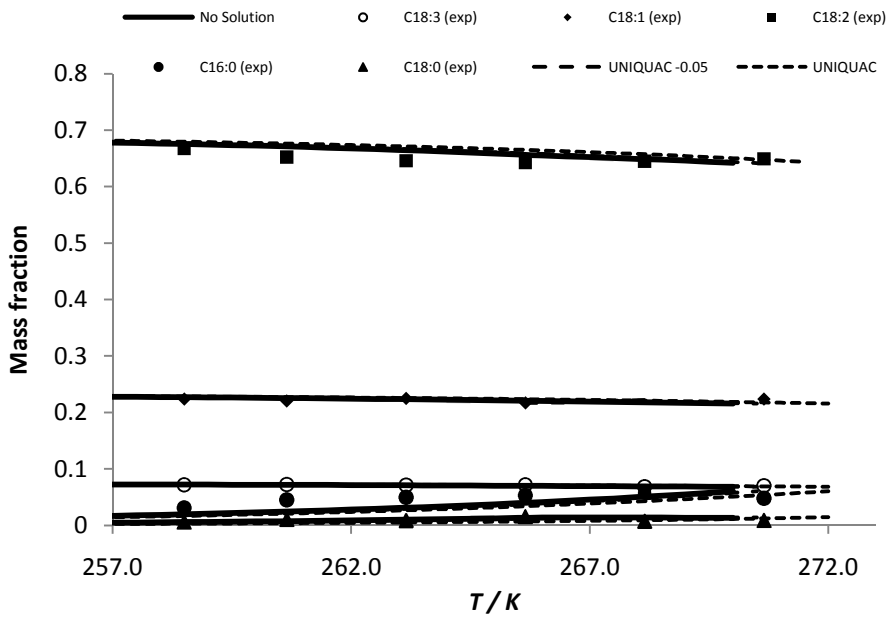

Figure 31-Liquid phase composition for biodiesel of rapeseed.

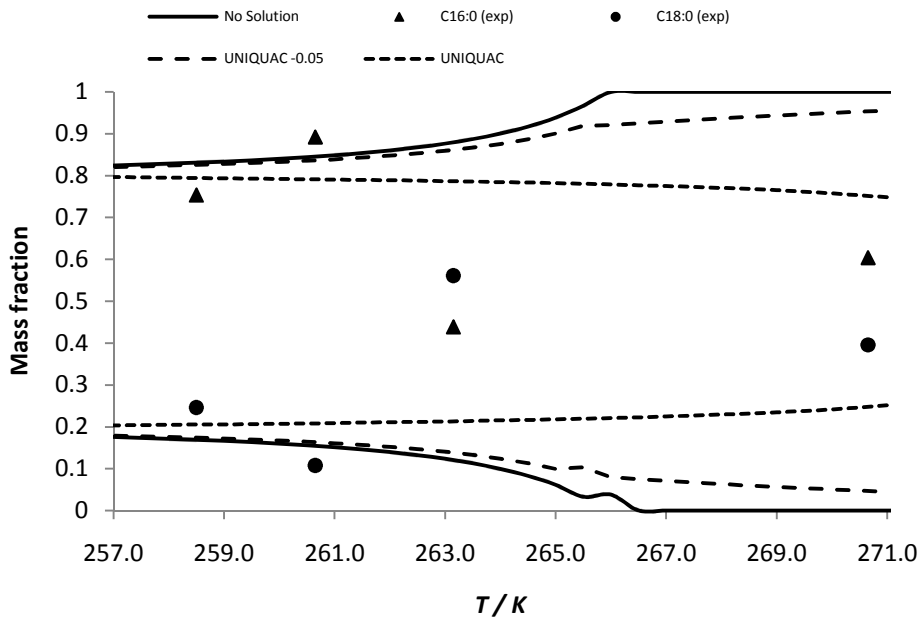

Figure 32-Solid phase composition for biodiesel of rapeseed.

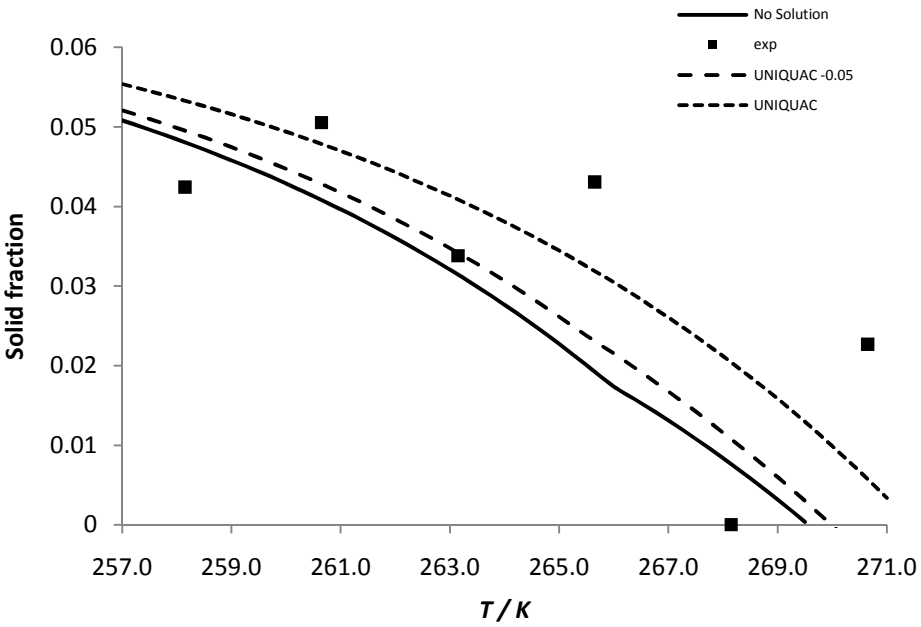

Figure 33-Dependence with temperature of the fraction of precipitated solid material for biodiesel of rapeseed.

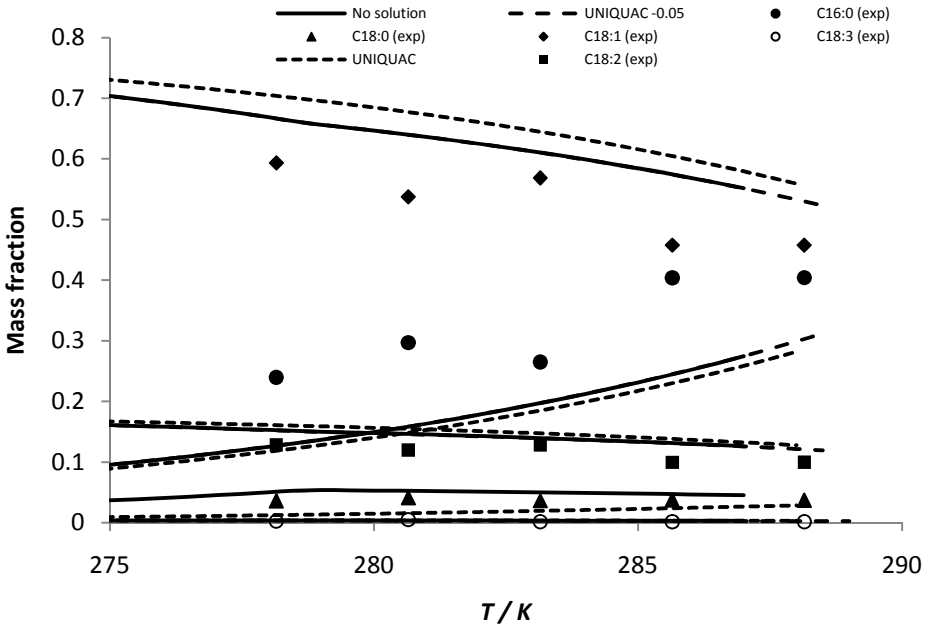

Figure 34-Liquid phase composition for biodiesel of palm.

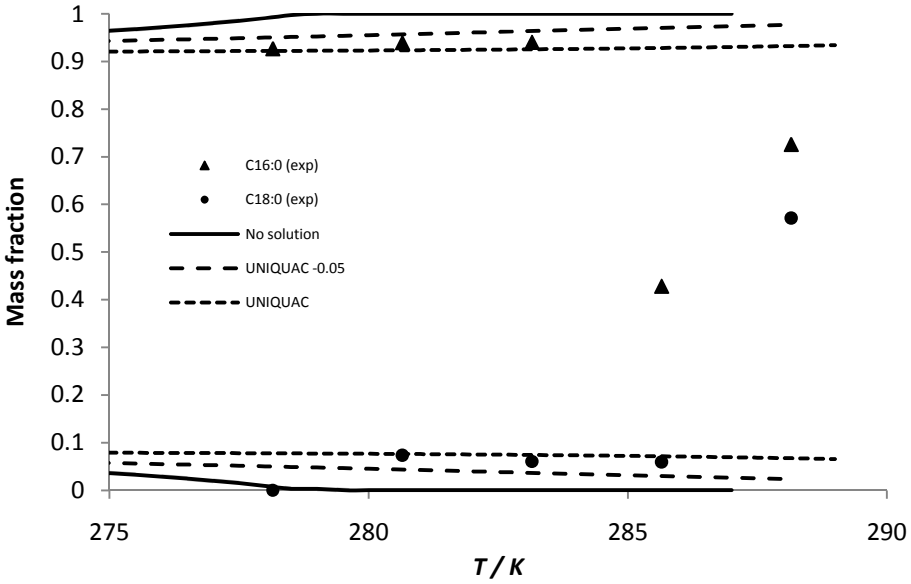

Figure 35-Solid phase composition for biodiesel of palm.

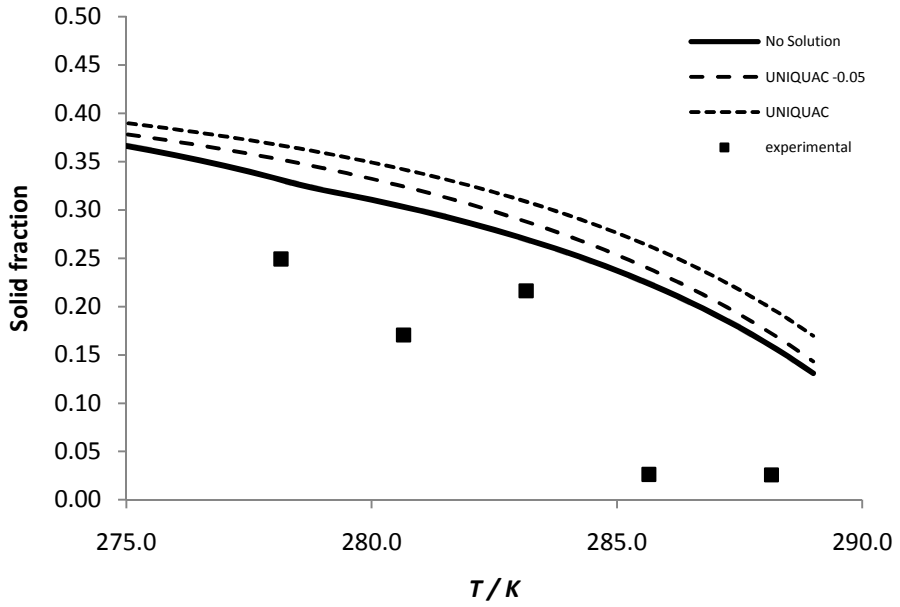

Figure 36-Dependence with temperature of the fraction of precipitated solid material for biodiesel of palm.

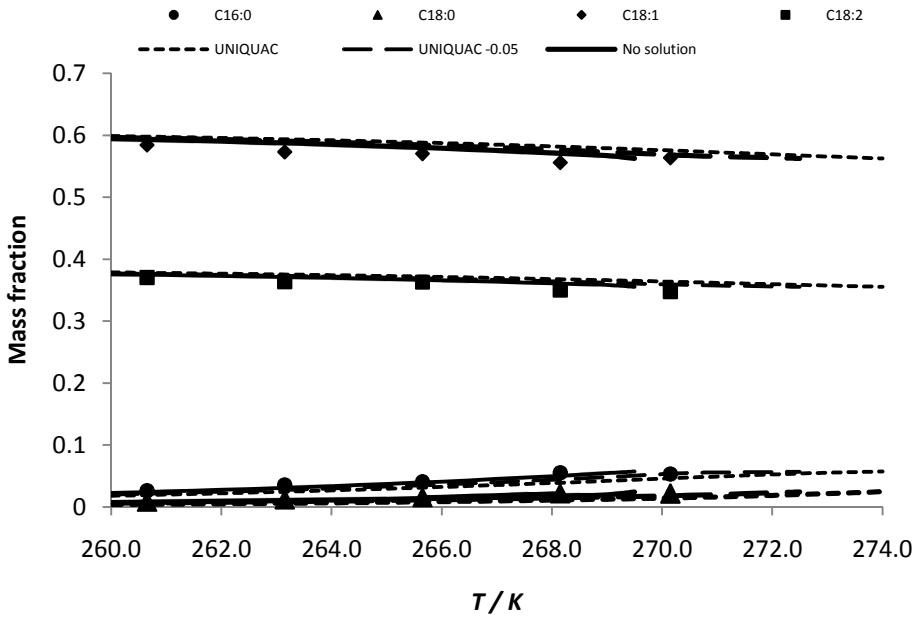

Figure 37-Liquid phase composition for BDA.

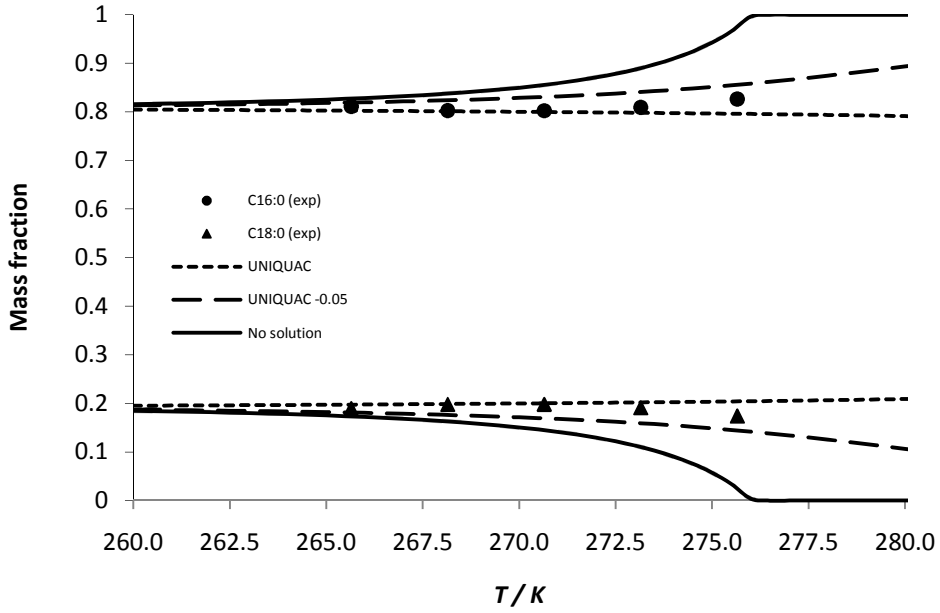

Figure 38-Solid phase composition for BDA.

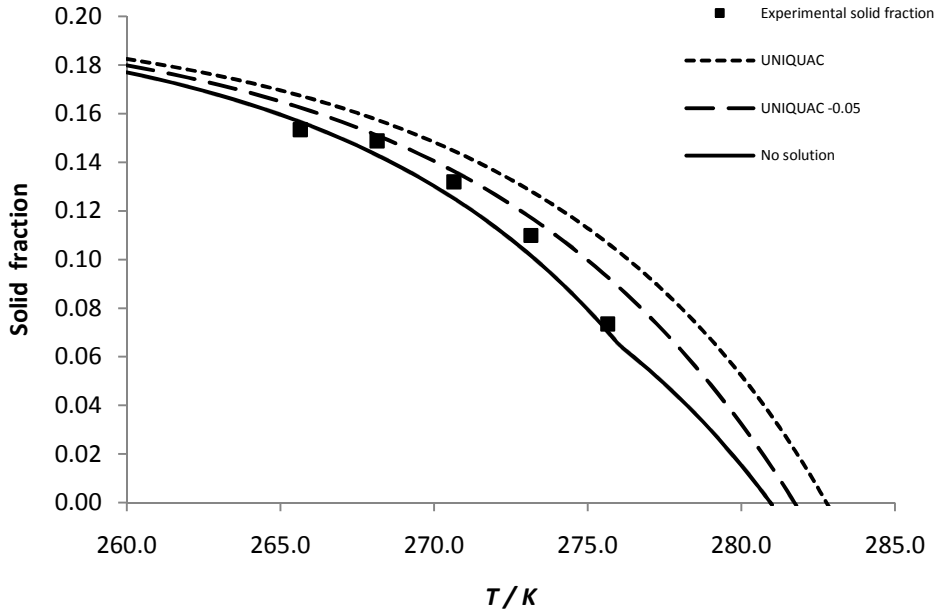

Figure 39-Dependence with temperature of the fraction of precipitated solid material for BDA.

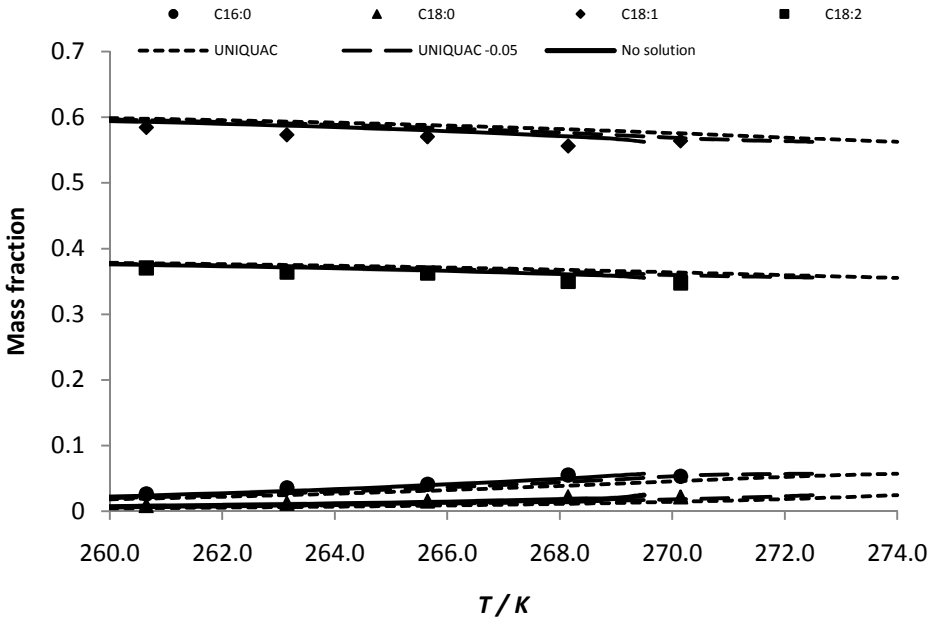

Figure 40-Liquid phase composition for BDB.

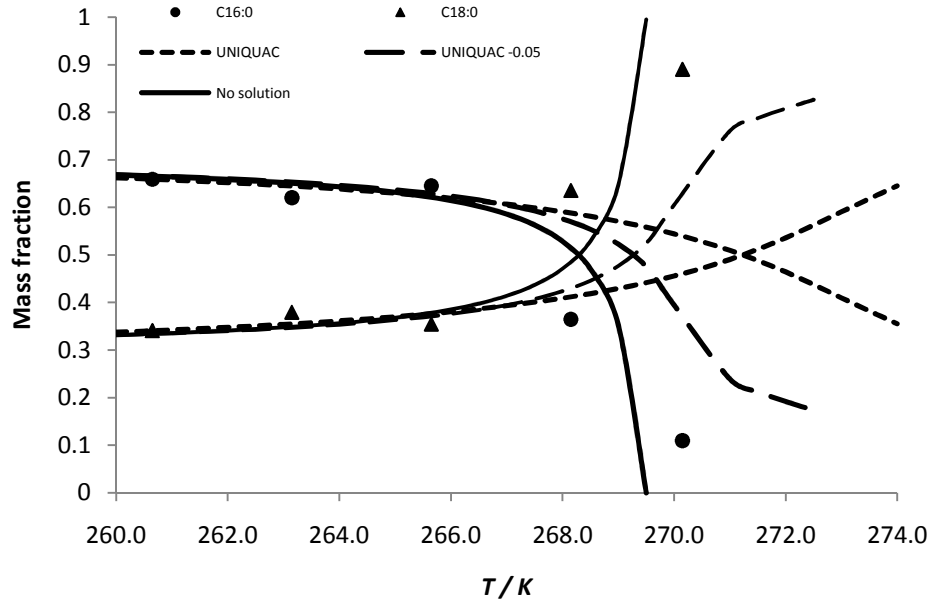

Figure 41-Solid phase composition for BDB.

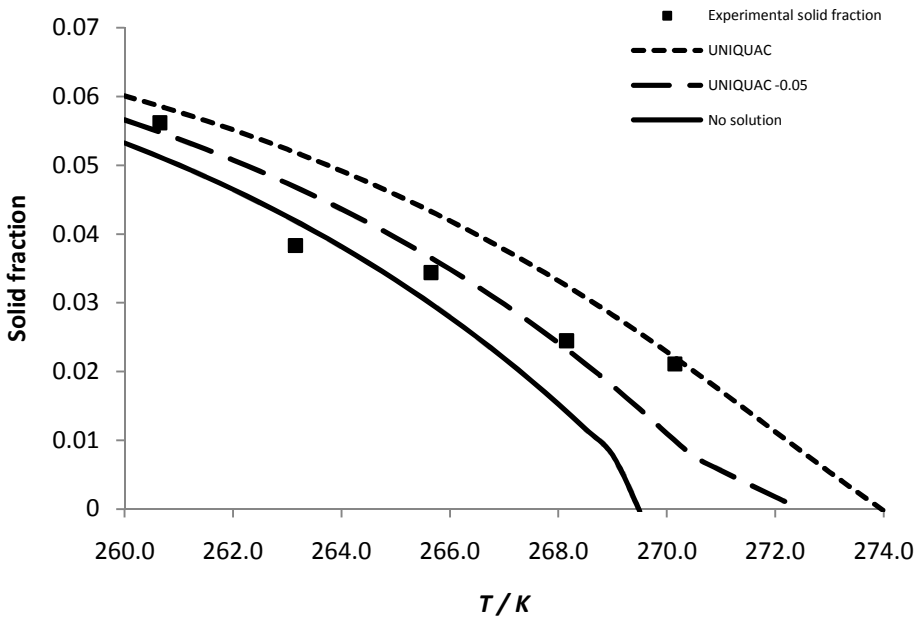

Figure 42-Dependence with temperature of the fraction of precipitated solid material for BDB.

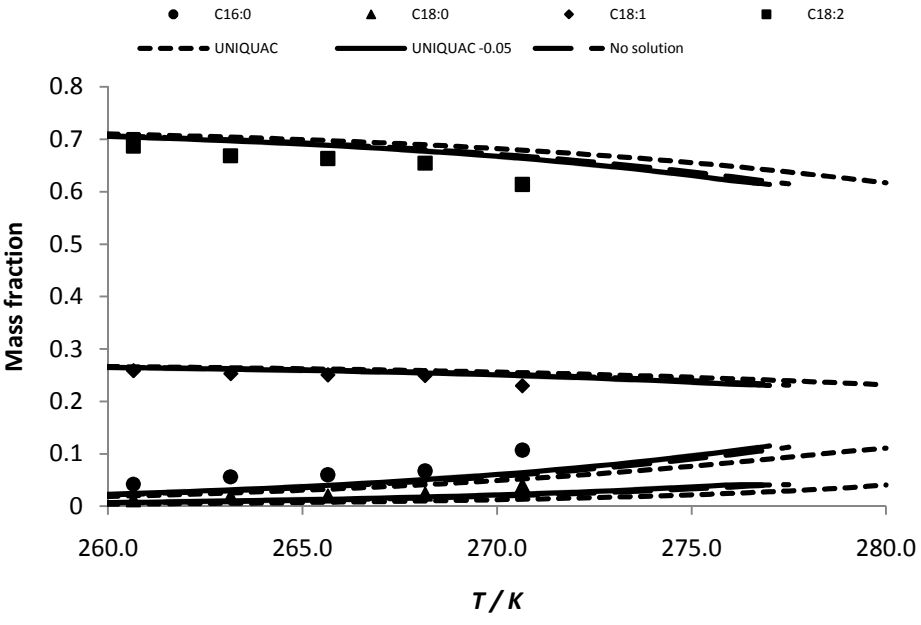

Figure 43-Liquid phase composition for BDC.

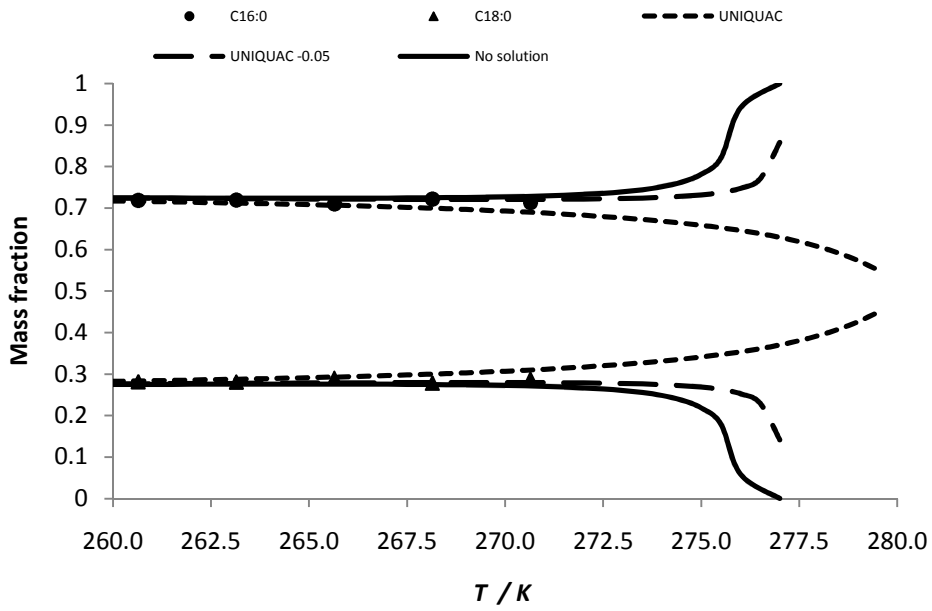

Figure 44-Solid phase composition for BDC.

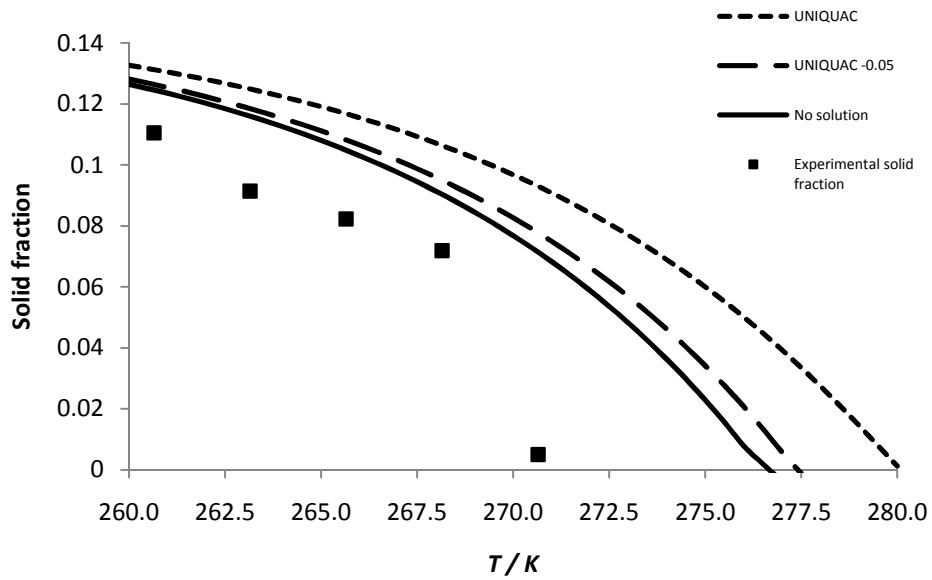

Figure 45-Dependence with temperature of the fraction of precipitated solid material for BDC.

The experimental methodology used on this work provides direct information about the composition of the liquid phase. The compositions of the solid phase are

estimated from the composition of the liquid phase and the precipitate according to Equations 6 and 7. The fraction of solids crystallizing from the biodiesel at each temperature is obtained from the differences between the concentrations of the unsaturated fatty acid esters on the original biodiesel and on the liquid phase according to Equation 8. It follows that the uncertainty associated with the solid phase compositions and the solid fractions is consequently larger than that of the liquid phase, which is just the uncertainty associated with the GC analysis.

Because the lowest temperatures studied here 257.5 K and 260.0 K and the melting points of the unsaturated fatty acids esters present on the biodiesel are lower than this value, it was admitted that these compounds did not crystallize under the conditions used in this work. The solid phase is thus composed solely by the saturated fatty acid methyl esters, methyl palmitate (C16:0) and methyl stearate (C18:0).

The temperature dependency of the liquid phase compositions observed for all of the biodiesel is similar, as show in Figure 28, Figure 31, Figure 34, Figure 37, Figure 40 and Figure 43. The major difference between the model and the experimental data is verified for biodiesel of palm that can be explained by the high level of saturated esters. As the temperatures decrease, the saturated esters crystallize and then the liquid phase becomes depleted on the saturated esters and enriched on the unsaturated esters. This results in an increase of the unsaturated esters concentration at low temperatures, while the saturated esters show the opposite behaviour with a decrease in the concentration with temperature. In what concerns the description of the liquid phase compositions, the three models adopted have quite similar performance, providing a description of the data that is essentially within their experimental uncertainty.

In Figure 29, Figure 32 and Figure 35 are presented the comparisons between experimental data obtained in this work and the models applied for solid phase. The results demonstrate that these models not provide a good description of the data. The high values obtained for the entrapped phase, c, indicate an inefficient separation of solid phase that can be explained by problems occurred during the experimental procedure, such as, an insufficient volume of biodiesel used in the syringes (in the final of the separation, a large dead volume remains inside of the syringes) or the porosity of filters of

the syringes to be insufficient to proceed at a good separation phase. The solid phase compositions presented in Figure 38, Figure 41 and Figure 44 represent the others similar systems considered in this work. These results present a richer and complex behaviour, being a stringent test to the models. Although the models predict a similar solid phase compositions at temperatures (5-10) K lower than the CP, close to it display a very different behaviour. While the predictive UNIQUAC model with $\alpha_{ij} = 0$ (UNIQUAC) predicts that both saturated esters crystallizes simultaneously, as expected from the formation of a solid solution, the model assuming that each esters crystallizes independently (no solution) starts with the crystallization of just one of the esters and, as the temperature decreases and the ratio between the stearate and palmitate esters reaches the eutectic point of the mixture, they both start to crystallize, although as independent solid phases. This produces some interesting features on the phase equilibrium predicted by the no solution model, such as a small increase on the concentration of the methyl stearate on the liquid phase below the CP and down to 276 K for BDA, while the methyl palmitate crystallizes alone.

In Figure 30, Figure 33, Figure 36, Figure 42 and Figure 45, shows the results for solid fraction. The solid fraction is directly affected by the solid phase so the inefficient separation of the phases that occurs in the case of biodiesel of soybean, rapeseed and palm explained the deviation between models and experimental results represented in Figure 30, Figure 33 and Figure 36. For other results represented in Figure 39, Figure 42 and Figure 45, it is possible observed that the crystallization will start bellow the CP.

The predictive UNIQUAC model with $\alpha_{ij} = -0.05$ (UNIQUAC – 0.05) presents an intermediate behaviour between these two extremes. In all cases, the solid fractions predicted by UNIQUAC model are larger than those estimated by the UNIQUAC – 0.05, and these are larger than those obtained from the no solution model. It is clear that the UNIQUAC model overestimates the solid fractions measurement. Given the quality of the experimental data measured for the solid fractions, it is not possible to clearly identify which of the two other models is the best because both describe the data within experimental uncertainly.

A global analysis of the data suggests that both the UNIQUAC – 0.05 and the no solution model can provide an adequate description of the phase equilibrium data of biodiesel below the CP of the fuel. The UNIQUAC – 0.05 model is probably superior, with a better description of the CP and the solid phase compositions.

4. Conclusions

Densities and viscosities of three biodiesels (soybean, rapeseed and palm), their blends and blends of these biodiesel with diesel fuel were measured as a function of temperature.

Experimental data demonstrate temperature dependence behaviour. For biodiesel blends, the results showing the variation of density and dynamic viscosity with temperature can be described by linear regressions with very good results. For biodiesel-diesel fuel blends were evaluated the influence of biodiesel concentration on such blends when mixed to diesel in 20, 40, 60 and 80 massic percentage. It was observed that the biodiesel leads to an increase in viscosity and density. According to the low values obtained for the difference between experimental and predictive data, it was found that simple mixing rules are suitable for predicting the basic properties of these blends in study.

The behaviour of biodiesel of soybean, rapeseed and palm were studied. A thermodynamic model was applied to describe this multiphase system and others similar systems obtained a previous work. Two versions of the predictive UNIQUAC model along with a model assuming complete immiscibility of the compounds in the solid phase are evaluated against the experimental data measured. It is shown that both the predictive UNIQUAC model with $\alpha_{ij} = -0.05$ (UNIQUAC -0.05) and a model assuming complete immiscibility on the solid phase are capable of providing an adequate representation of the phase equilibrium for these systems bellow their CPs.

5. References

1. Demirbas, A., *Importance of biodiesel as transportation fuel.* Energy Policy, 2007. **35**(9): p. 4661-4670.

2. Benjumea, P., J. Agudelo, and A. Agudelo, *Basic properties of palm oil biodiesel-diesel blends.* Fuel, 2008. **87**(10-11): p. 2069-2075.

3. Harumi Veny, S.B., Mohamed Kheireddine Aroua , Masitah Hasan, Abdul Aziz Raman1 and Nik Meriam Nik Sulaiman, *Density of Jatropha curcas Seed Oil and its Methyl Esters: Measurement and Estimations* International Journal of Thermophysics, 2009. **30**(2): p. 529-541.

4. Lopes, J.C.A., L. Boros, M.A. Krähenbühl, A.J.A. Meirelles, J.L. Daridon, J. Pauly, I.M. Marrucho, and J.A.P. Coutinho, *Prediction of Cloud Points of Biodiesel†.* Energy & Fuels, 2007. **22**(2): p. 747-752.

5. Boros, L., M.L.S. Batista, R.V. Vaz, B.R. Figueiredo, V.F.S. Fernandes, M.C. Costa, M.A. Krahonbuhl, A.J.A. Meirelles, and J.A.P. Coutinho, *Crystallization Behavior of Mixtures of Fatty Acid Ethyl Esters with Ethyl Stearate.* Energy & Fuels, 2009. **23**: p. 4625-4629.

6. J. C. A. Lopes, L.B., § M. A. Krähenbühl, A. J. A. Meirelles,| J. L. Daridon, and I.M.M. J. Pauly, and J. A. P. Coutinho, *Prediction of Cloud Points of Biodiesel.* 2007.

7. Ma, W.X.a.N., *Immobilized Lipase on Fe_3O_4 Nanoparticles as Biocatalyst for Biodiesel Production.* Energy & Fuels, 2009. **23**: p. 1347-1353.

8. Nielsen, P.M., J. Brask, and L. Fjerbaek, *Enzymatic biodiesel production: Technical and economical considerations.* European Journal of Lipid Science and Technology, 2008. **110**(8): p. 692-700.

9. Veena Kumari, S.S., and Munishwar N. Gupta, *Preparation of Biodiesel by Lipase-Catalyzed Transesterification of High Free Fatty Acid Containing Oil from Madhuca indica.* Energy & Fuels, 2006. **21**: p. 368-372.

10. Candeia, R.A., M.C.D. Silva, J.R. Carvalho Filho, M.G.A. Brasilino, T.C. Bicudo, I.M.G. Santos, and A.G. Souza, *Influence of soybean biodiesel content on basic properties of biodiesel-diesel blends.* Fuel, 2009. **88**(4): p. 738-743.

11. Cardona, C.A. and Ó.J. Sánchez, *Fuel ethanol production: Process design trends and integration opportunities.* Bioresource Technology, 2007. **98**(12): p. 2415-2457.

12. Mehta, G.D. and M.D. Fraser, *A novel extraction process for separating ethanol and water.* Industrial & Engineering Chemistry Process Design and Development, 1985. **24**(3): p. 556-560.

13. Vane, L.M., *Separation technologies for the recovery and dehydration of alcohols from fermentation broths.* Biofuels, Bioproducts and Biorefining, 2008. **2**(6): p. 553-588.

14. Parawira, W., *Biotechnological production of biodiesel fuel using biocatalysed transesterification: A review.* Critical Reviews in Biotechnology, 2009. **29(2)**: p. 82-93.

15. Lestari, S., P. Maki-Arvela, J. Beltramini, G.Q.M. Lu, and D.Y. Murzin, *Transforming Triglycerides and Fatty Acids into Biofuels.* ChemSusChem, 2009. **2**(12): p. 1109-1119.

16. Fjerbaek, L., K.V. Christensen, and B. Norddahl, *A Review of the Current State of Biodiesel Production Using Enzymatic Transesterification.* Biotechnology and Bioengineering, 2009. **102**(5): p. 1298-1315.

17. Kiss, A.A., A.C. Dimian, and G. Rothenberg, *Solid acid catalysts for biodiesel production - Towards sustainable energy.* Advanced Synthesis & Catalysis, 2006. **348**(1-2): p. 75-81.

18. Qi, D.H., H. Chen, L.M. Geng, Y.Z. Bian, and X.C. Ren, *Performance and combustion characteristics of biodiesel-diesel-methanol blend fuelled engine.* Applied Energy, 2010. **87**(5): p. 1679-1686.

19. http://www.propelbiofuels.com/site/aboutbiodiesel.html. Consulted: 18 of June, 2010.

20. Majer, S., F. Mueller-Langer, V. Zeller, and M. Kaltschmitt, *Implications of biodiesel production and utilisation on global climate - A literature review.* European Journal of Lipid Science and Technology, 2009. **111**(8): p. 747-762.

21. Diário da República, Portaria n.º69/2010, 4 de Fevereiro de 2010.

22. Rodrigues, R.C., G. Volpato, K. Wada, and M.A.Z. Ayub, *Enzymatic synthesis of biodiesel from transesterification reactions of vegetable oils and short chain alcohols.* Journal of the American Oil Chemists Society, 2008. **85**(10): p. 925-930.

23. Dalla Rosa, C., M.B. Morandim, J.L. Ninow, D. Oliveira, H. Treichel, and J.V. Oliveira, *Continuous lipase-catalyzed production of fatty acid ethyl esters from soybean oil in compressed fluids.* Bioresource Technology, 2009. **100**(23): p. 5818-5826.

24. Mukesh Kumar Modi, J.R.C.R., B. V. R. K. Rao & R. B. N. Prasad, *Lipase-mediated transformation of vegetable oils into biodiesel using propan-2-ol as acyl acceptor.* Biotechnology Letters, 2006. **28**: p. 637-640.

25. Oliveira, M.B., A.R.R. Teles, A.J. Queimada, and J.A.P. Coutinho, *Phase equilibria of glycerol containing systems and their description with the Cubic-Plus-Association (CPA) Equation of State.* Fluid Phase Equilibria, 2009. **280**(1-2): p. 22-29.

26. C. R. Krishna, K.T., Christopher Brown, Thomas A. Butcher, and a.D.M. Mouzhgun Anjom, *Cold Flow Behavior of Biodiesels Derived from Biomass Sources.* 2009.

27. J.M. Marchetti, V.U.M., A.F. Errazu (2005) *Possible methods for biodiesel production*.

28. Al-Zuhair, S., *Production of biodiesel: possibilities and challenges.* Biofuels Bioproducts & Biorefining-Biofpr, 2007. **1**(1): p. 57-66.

29. Akoh, C.C., S.W. Chang, G.C. Lee, and J.F. Shaw, *Enzymatic approach to biodiesel production.* Journal of Agricultural and Food Chemistry, 2007. **55**(22): p. 8995-9005.

30. Srivathansan Vembanur Ranganathan, S.L.N., Karuppan Muthukumar, *An overview of enzymatic production of Biodiesel.* Bioresource Technology, 2008. **99**: p. 3975-3981.

31. Adamczak, M., U.T. Bornscheuer, and W. Bednarski, *The application of biotechnological methods for the synthesis of biodiesel.* European Journal of Lipid Science and Technology, 2009. **111**(8): p. 800-813.

32. Guang Jin, T.J.B., Christopher G. Hamaker, Robert Rhykerd and Lucy A. Loftus, *Production biodiesel using whole-cell biocatalysts in separate hydrolysis and methanolysis reactions.* Journal of Environmental Science and Health, 2008. **Part A 43**: p. 589-595.

33. Yori, J.C., S.A. D'Ippolito, C.L. Pieck, and C.R. Vera, *Deglycerolization of Biodiesel Streams by Adsorption Over Silica Beds.* Energy & Fuels, 2006. **21**(1): p. 347-353.

34. Hájek, M. and F. Skopal, *Treatment of glycerol phase formed by biodiesel production.* Bioresource Technology, 2010. **101**(9): p. 3242-3245.

35. H. Noureddini, X.G., R.S. Philkana, *Immobilized Pseudomonas cepacia lipase for biodiesel fuel production from soybean oil.* Bioresource Technology, 2005. **96**: p. 769-777.

36. Mamoru Iso, B.C., Masashi Eguchi, Takashi Kudo, Surekha Shrestha, *Production of biodiesel fuel from tryglycerides and alcohol using immobilized lipase.* Journal of Molecular Catalysis B, 2001. **Enzymatic 16**: p. 53-58.

37. C. Dalla Rosa, M.B.M., J. L. Ninow, D. Oliveira, H. Treichel, J. Vladimir Oliveira, *Lipase-catalyzed production of fatty acid ethyl esters from soybean oil in compressed propane.* Journal of Supercritical Fluids 2008. **47**: p. 49-53.

38. Babu, I.S.a.R., Garapati Hanumantha, *Lipase Production by Yarrowia lipolytica NCIM 3589 in Solid State Fermentation Using Mixed Substrate.* Journal of Microbiology 2, 2007. **5**: p. 469-474.

39. Dong Hwan Lee, J.M.L., Hyun Young Shin, Seong Woo Kang, and Seung Wook Kim, *Biodiesel Production Using a Mixture of Immobilized Rhizopus oryzae and Candida rugosa Lipases.* Biotechnology and Bioprocess Engineering, 2006. **11**: p. 522-525.

40. Asha Chaubey, R.P., Surrinder Koul, Subhash C. Taneja, Ghulam N. Qazi, *Arthrobacter sp. lipase immobilization for improvement in stability and enantioselectivity.* Appl Microbiol Biotechnol, 2006. **73**: p. 598-606.

41. Baroutian, S., M.K. Aroua, A.A.A. Raman, and N.M.N. Sulaiman, *Viscosities and Densities of Binary and Ternary Blends of Palm Oil + Palm Biodiesel + Diesel Fuel at Different Temperatures.* Journal of Chemical & Engineering Data, 2009. **55**(1): p. 504-507.

42. Baroutian, S., M.K. Aroua, A.A.A. Raman, and N.M.N. Sulaiman, *Densities of Ethyl Esters Produced from Different Vegetable Oils.* Journal of Chemical & Engineering Data, 2008. **53**(9): p. 2222-2225.

43. Baroutian, S., M.K. Aroua, A.A.A. Raman, and N.M.N. Sulaiman, *Density of Palm Oil-Based Methyl Ester.* Journal of Chemical & Engineering Data, 2008. **53**(3): p. 877-880.

44. BS*, EN 14214 Automotive fuels - Fatty acid methyl esters (FAME) for diesel engines - Requirements and test methods. 2009.*

45. Smith, P.C., Y. Ngothai, Q. Dzuy Nguyen, and B.K. O'Neill, *Improving the low-temperature properties of biodiesel: Methods and consequences.* Renewable Energy, 2010. **35**(6): p. 1145-1151.

46. Bagby, M.O., Dunn, R. O., Shockley, M. W., *Improving the Low-Temperature Properties of Alternative Diesel Fuels: Vegetable Oil-Derived Methyl Esters.* 1996. **73**.

47. Mirante, F., *Caracterização por GC-MS de óleos vegetais e ceras parafínicas*, in *Departamento de Química*. 2007, Universidade de Aveiro: Aveiro.

48. Moore, W.J., ed. *Physical Chemistry*. 1972, Prentice-Hall: New Jersey.

49. Hoyt, C.S. and C.K. Fink, *The Constants of Ebullioscopy.* The Journal of Physical Chemistry, 1937. **41**(3): p. 453-456.

50. Grunberg, L.a.A.H.N., *Mixture Law for Viscosity.* Nature, 1949. **164**: p. 799–800.

51. Blangino E., A.F.R., S. D. Romano, *Numerical expressions for viscosity, surface tension and density of biodiesel: analysis and experimental validation.* Physics and Chemistry of Liquids, 2008. **46**: p. 527-547.

52. Yuan, W., A.C. Hansen, and Q. Zhang, *Predicting the temperature dependent viscosity of biodiesel fuels.* Fuel, 2009. **88**(6): p. 1120-1126.

53. Cheng Sit Foon, Y.C.L., Noor Lida Habi Mat Dian, Choo Yuen May and C.C.H.a.M.A. Ngan, *Crystallisation and Melting Behavior of Methyl Esters of Palm Oil.* American Journal of Applied Sciences 2006. **3**(5): p. 1859-1863.

54. Coutinho, J.A.P. and V. RuffierMeray, *Experimental measurements and thermodynamic modeling of paraffinic wax formation in undercooled solutions.* Industrial & Engineering Chemistry Research, 1997. **36**(11): p. 4977-4983.

55. Dauphin, C., J.L. Daridon, J.A.P. Coutinho, P. Baylere, and M. Potin-Gautier, *Wax content measurements in partially frozen paraffinic systems.* Fluid Phase Equilibria, 1999. **161**(1): p. 135-151.

56. Pauly, J., J.L. Daridon, and J.A.P. Coutinho, *Measurement and prediction of temperature and pressure effect on wax content in a partially frozen paraffinic system.* Fluid Phase Equilibria, 2001. **187**: p. 71-82.

57. Pauly, J., J.-L. Daridon, and J.A.P. Coutinho, *Solid deposition as a function of temperature in the nC10 + (nC24-nC25-nC26) system.* Fluid Phase Equilibria, 2004. **224**(2): p. 237-244.

58. Pauly, J., J.-L. Daridon, J.A.P. Coutinho, and M. Dirand, *Crystallisation of a multiparaffinic wax in normal tetradecane under high pressure.* Fuel, 2005. **84**(4): p. 453-459.

59. Coutinho, J.A.P., C. Goncalves, I.M. Marrucho, J. Pauly, and J.L. Daridon, *Paraffin crystallization in synthetic mixtures: Predictive local composition models revisited.* Fluid Phase Equilibria, 2005. **233**(1): p. 28-33.

60. Coutinho, J.A.P., K. Knudsen, S.I. Andersen, and E.H. Stenby, *A local composition model for paraffinic solid solutions.* Chemical Engineering Science, 1996. **51**(12): p. 3273-3282.

61. Coutinho, J.A.P. and E.H. Stenby, *Predictive Local Composition Models for Solid/Liquid Equilibrium in n-Alkane Systems: Wilson Equation for Multicomponent Systems.* Industrial & Engineering Chemistry Research, 1996. **35**(3): p. 918-925.

62. Coutinho, J.A.P., *Predictive UNIQUAC: A New Model for the Description of Multiphase Solid−Liquid Equilibria in Complex Hydrocarbon Mixtures.* Industrial & Engineering Chemistry Research, 1998. **37**(12): p. 4870-4875.

63. Coutinho, J.A.P., F. Mirante, and J. Pauly, *A new predictive UNIQUAC for modeling of wax formation in hydrocarbon fluids.* Fluid Phase Equilibria, 2006. **247**(1-2): p. 8-17.

64. Coutinho, J.A.P., C. Dauphin, and J.L. Daridon, *Measurements and modelling of wax formation in diesel fuels.* Fuel, 2000. **79**(6): p. 607-616.

65. Coutinho, J.A.P., *A Thermodynamic Model for Predicting Wax Formation in Jet and Diesel Fuels.* Energy & Fuels, 2000. **14**(3): p. 625-631.

66. Pauly, J., J.-L. Daridon, J.-M. Sansot, and J.A.P. Coutinho, *The pressure effect on the wax formation in diesel fuel[small star, filled].* Fuel, 2003. **82**(5): p. 595-601.

67. Mirante, F.I.C. and J.A.P. Coutinho, *Cloud point prediction of fuels and fuel blends.* Fluid Phase Equilibria, 2001. **180**(1-2): p. 247-255.

68. Coutinho, J.A.P., F. Mirante, J.C. Ribeiro, J.M. Sansot, and J.L. Daridon, *Cloud and pour points in fuel blends.* Fuel, 2002. **81**(7): p. 963-967.

69. Queimada, A.J.N., C. Dauphin, I.M. Marrucho, and J.A.P. Coutinho, *Low temperature behaviour of refined products from DSC measurements and their thermodynamical modelling.* Thermochimica Acta, 2001. **372**(1-2): p. 93-101.

70. Coutinho, J.A.P. and J.-L. Daridon, *Low-Pressure Modeling of Wax Formation in Crude Oils.* Energy & Fuels, 2001. **15**(6): p. 1454-1460.

71. Jean-Marc Sansot, J.P., Jean-Luc Daridon, Joao A. P. Coutinho, *Modeling High-Pressure Wax Formation in Petroleum Fluids*. 2005, AIChe Journal. p. 2089-2097.

72. Coutinho, J.A.P., B. Edmonds, T. Moorwood, R. Szczepanski, and X. Zhang, *Reliable Wax Predictions for Flow Assurance.* Energy & Fuels, 2006. **20**(3): p. 1081-1088.

73. Coutinho, J.A.P., *Predictive local composition models: NRTL and UNIQUAC and their application to model solid-liquid equilibrium of n-alkanes.* Fluid Phase Equilibria, 1999. **158-160**: p. 447-457.

74. Daridon, J.-L., J. Pauly, J.A.P. Coutinho, and F. Montel, *Solid−Liquid−Vapor Phase Boundary of a North Sea Waxy Crude: Measurement and Modeling.* Energy & Fuels, 2001. **15**(3): p. 730-735.

75. Costa, M.C., M.A. Krähenbühl, A.J.A. Meirelles, J.L. Daridon, J. Pauly, and J.A.P. Coutinho, *High pressure solid-liquid equilibria of fatty acids.* Fluid Phase Equilibria, 2007. **253**(2): p. 118-123.

76. Lopes, J.C.A., L. Boros, M.A. Krahenbuhl, A.J.A. Meirelles, J.L. Daridon, J. Pauly, I.M. Marrucho, and J.A.P. Coutinho, *Prediction of cloud points of biodiesel.* Energy & Fuels, 2008. **22**(2): p. 747-752.

77. J. M. Prausnitz, R.N.L., E. G. Azevedo, ed. *Molecular Thermodynamics of Fluid-Phase Equilibria*. 3 rd ed. 1999, Pretince Hall: New York.

78. Coutinho, J.A.P., S.I. Andersen, and E.H. Stenby, *Evaluation of activity coefficient models in prediction of alkane solid-liquid equilibria.* Fluid Phase Equilibria, 1995. **103**(1): p. 23-39.

79. Leibovici, C.F. and J. Neoschil, *A solution of Rachford-Rice equations for multiphase systems.* Fluid Phase Equilibria, 1995. **112**(2): p. 217-221.

80. Larsen, B.L., P. Rasmussen, and A. Fredenslund, *A modified UNIFAC group-contribution model for prediction of phase equilibria and heats of mixing.* Industrial & Engineering Chemistry Research, 1987. **26**(11): p. 2274-2286.

81. D. S. Abrams, J.M.P., *Statistical Thermodynamics of Liquid Mixtures: A New Expression for the Excess Gibbs Energy of Partly or Completely Miscible Systems.* AIChE Journal, 1975. **21**(1): p. 116-128.

82. Coutinho, J.o.A.P., M. Gonçalves, M.J. Pratas, M.L.S. Batista, V.F.S. Fernandes, J. Pauly, and J.L. Daridon, *Measurement and Modeling of Biodiesel Cold-Flow Properties.* Energy & Fuels, 2010. **24**(4): p. 2667-2674.

83. Dzida, M. and P. Prusakiewicz, *The effect of temperature and pressure on the physicochemical properties of petroleum diesel oil and biodiesel fuel.* Fuel, 2008. **87**(10-11): p. 1941-1948.

84. Yoon, S.H., S.H. Park, and C.S. Lee, *Experimental Investigation on the Fuel Properties of Biodiesel and Its Blends at Various Temperatures.* Energy & Fuels, 2007. **22**(1): p. 652-656.

Appendix A

Transesterification reaction/ Purification Step

A mass of the alkaline catalyst, potassium hydroxide pure, was added in absolute methanol and shaken until dissolved. This solution was then mixed with oil in a round-bottom flask with a capacity of the 500 mL. This round-bottom flask was previously dipped in a hot water bath at 45ºC and a magnetic stirrer was used to promote a homogeneous mixture. The reaction temperature was controlled by an immersion circulator. After 45 minutes of the reaction, the mixture was transferred to a separating funnel. The two layers, biodiesel (top) and glycerol (bottom) were separated by sedimentation. Glycerol was removed and biodiesel was washed with distillate hot water three times, until neutral pH was achieved. The excess of water was removed from biodiesel by filtration with pure sodium sulphate anhydrous. The amount of reagents used to reaction was in Table A1.

Table A1-Masses of reagents used to transesterification reaction.

	BD Palm	BD Soybean	BD Rapeseed
m_{NaOH} ± 0.00005 / g	0.4008	0.4041	0.4060
m_{oil} ± 0.00005 / g	80.0610	80.0736	80.0480
V_{MeOH} ± 0.25 / mL	16.00	16.00	16.00

Table A2 –Percentage of saturated and unsaturated fatty acids presents in biodiesels.

wt %	BD Soybean	BD Rapeseed	BD Palm
Saturated	14.11	7.14	45.02
Unsaturated	85.89	92.86	54.98

Appendix B

Table B1- Masses of biodiesels used to prepared blends.

	49.63% BD Rapeseed+50.38% BD Soybean	49.89% BD Rapeseed+50.11% BD Palm	49.89% BD Rapeseed+50.11% BD Soybean	33.36% BD Soybean+ 33.38% BD Palm+33.26% BD Rapeseed
$m_{BD\ Rapeseed}$ / g	1.8316	1.7871	---------	1.2699
$m_{BD\ Soybean}$ / g	1.8596	---------	1.6957	1.2737
$m_{BD\ Palm}$ / g	---------	1.7948	1.7033	1.2742

Table B2 –Dynamic viscosity and density with the associated standard deviation for the biodiesel of palm at different temperatures.

T / K	Viscosity / mPa.s	$\sigma_{viscosity}$	Density / g.cm^{-3}	$\sigma_{Density}$
293.15	9.3764	0.091	0.8815	0.00006
298.15	8.0818	0.083	0.8778	0
303.15	7.0221	0.074	0.8741	0
308.15	6.1524	0.064	0.8705	0.00006
313.15	5.4313	0.052	0.8668	0.00006
318.15	4.8266	0.042	0.8632	0.00006
323.15	4.3152	0.035	0.8595	0.00016
328.15	3.8797	0.027	0.8559	0.00006
333.15	3.5039	0.020	0.8523	0.00006
338.15	3.1816	0.014	0.8487	0.00006
343.15	2.9021	0.010	0.8450	0
348.15	2.6570	0.0054	0.8414	0
353.15	2.4429	0.0043	0.8378	0
358.15	2.2551	0.0036	0.8342	0
363.15	2.0885	0.0030	0.8306	0

Table B3-Dynamic viscosity and density with the associated standard deviation for biodiesel of rapeseed at different temperatures.

T / K	Viscosity / mPa.s	$\sigma_{viscosity}$	Density / g.cm^{-3}	$\sigma_{Density}$
283.15	10.4710	0.0014	0.8920	0.00007
288.15	8.9333	0.0067	0.8883	0
293.15	7.6988	0.0020	0.8846	0
298.15	6.6954	0.0028	0.8810	0
303.15	5.8735	0.0018	0.8774	0
308.15	5.1929	0.00021	0.8737	0
313.15	4.6222	0.000000	0.8701	0.00007
318.15	4.1397	0.00021	0.8665	0.00007
323.15	3.7285	0.00071	0.8628	0.0001
328.15	3.3754	0.0016	0.8592	0.0001
333.15	3.0701	0.0025	0.8556	0.00007
338.15	2.8057	0.0023	0.8519	0.0001
343.15	2.5738	0.0036	0.8483	0.00007
348.15	2.3693	0.0044	0.8446	0.00007
353.15	2.1897	0.0041	0.8409	0.00000
358.15	2.0298	0.0040	0.8374	0.00007
363.15	1.8872	0.0039	0.8338	0

Table B4–Dynamic viscosity and density with the associated standard deviation for biodiesel of soybean at different temperatures.

-T / K	Viscosity / mPa.s	$\sigma_{viscosity}$	Density / g.cm^{-3}	$\sigma_{Density}$
283.15	12.0705	0.033	0.8982	0.0002
288.15	10.2820	0.042	0.8945	0.0002
293.15	8.8451	0.045	0.8909	0.0002
298.15	7.6788	0.044	0.8873	0.0002
303.15	6.7248	0.045	0.8836	0.0001
308.15	5.9339	0.045	0.8800	0.0001
313.15	5.2731	0.039	0.8764	0.0002
318.15	4.7056	0.032	0.8728	0.00007
323.15	4.2280	0.028	0.8692	0.00007
328.15	3.8194	0.024	0.8656	0
333.15	3.4612	0.020	0.8620	0
338.15	3.1576	0.020	0.8584	0.00007
343.15	2.8919	0.019	0.8548	0.00007
348.15	2.6537	0.012	0.8512	0.00007
353.15	2.4411	0.0030	0.8476	0.00007
358.15	2.2517	0.0023	0.8441	0.00007
363.15	2.0872	0.0025	0.8406	0.00007

Table B5–Dynamic viscosity and density with the associated standard deviation for binary blend, biodiesel of soybean and rapeseed in equal massic percentage as a function of temperature.

T / K	Viscosity / mPa.s	$\sigma_{viscosity}$	Density / g.cm^{-3}	$\sigma_{Density}$
283.15	11.2240	0.097	0.8963	0.0003
288.15	9.5612	0.077	0.8926	0.0003
293.15	8.2365	0.064	0.8890	0.0003
298.15	7.1600	0.052	0.8853	0.0003
303.15	6.2804	0.044	0.8816	0.0002
308.15	5.5475	0.041	0.8780	0.0002
313.15	4.9367	0.032	0.8744	0.0002
318.15	4.4213	0.025	0.8708	0.0002
323.15	3.9825	0.021	0.8671	0.0002
328.15	3.6051	0.017	0.8635	0.0002
333.15	3.2794	0.014	0.8599	0.0002
338.15	2.9968	0.012	0.8563	0.0002
343.15	2.7493	0.010	0.8527	0.0002
348.15	2.5311	0.0088	0.8491	0.0002
353.15	2.3390	0.0079	0.8455	0.0002
358.15	2.1675	0.0066	0.8419	0.0002
363.15	2.0145	0.0056	0.8383	0.0001

Table B6–Dynamic viscosity and density with the associated standard deviation for binary blend, biodiesel of rapeseed and palm in equal massic percentage as a function of temperature.

T / K	Viscosity / mPa.s	$\sigma_{viscosity}$	Density / g.cm^{-3}	$\sigma_{Density}$
293.15	8.5263	0.024	0.8835	0.0001
298.15	7.3792	0.020	0.8798	0.00006
303.15	6.4477	0.017	0.8762	0.00006
308.15	5.6720	0.014	0.8725	0.00006
313.15	5.0263	0.011	0.8689	0.00006
318.15	4.4849	0.0095	0.8652	0.00006
323.15	4.0257	0.0080	0.8616	0.00006
328.15	3.6343	0.0085	0.8580	0.00006
333.15	3.2955	0.0060	0.8543	0.00006
338.15	3.0024	0.0048	0.8507	0.00006
343.15	2.7466	0.0034	0.8471	0.00006
348.15	2.5229	0.0029	0.8435	0
353.15	2.3258	0.0023	0.8399	0
358.15	2.1514	0.0021	0.8363	0
363.15	1.9964	0.0018	0.8327	0

Table B7–Dynamic viscosity and density with the associated standard deviation for binary blend, biodiesel of rapeseed and palm in equal massic percentage as a function of temperature.

T / K	Viscosity / mPa.s	$\sigma_{viscosity}$	Density / g.cm^{-3}	$\sigma_{Density}$
293.15	8.9831	0.23	0.8868	0.00006
298.15	7.7809	0.18	0.8831	0.00006
303.15	6.7992	0.15	0.8795	0
308.15	5.9840	0.12	0.8759	0
313.15	5.3046	0.099	0.8723	0
318.15	4.7313	0.081	0.8687	0.00006
323.15	4.2455	0.065	0.8650	0.00006
328.15	3.8309	0.053	0.8614	0.00006
333.15	3.4689	0.038	0.8578	0.00006
338.15	3.1559	0.026	0.8541	0.0001
343.15	2.8870	0.021	0.8505	0.0001
348.15	2.6524	0.020	0.8469	0.0001
353.15	2.4459	0.017	0.8433	0.0001
358.15	2.2691	0.0073	0.8397	0.0001
363.15	2.1072	0.0082	0.8361	0.0001

Table B8 – Dynamic viscosity and density with the associated standard deviation for ternary blend, biodiesel of rapeseed, palm and soybean in equal massic percentage as a function of temperature.

T / K	Viscosity / mPa.s	$\sigma_{viscosity}$	Density / g.cm^{-3}	$\sigma_{Density}$
293.15	8.6648	0.025	0.8862	0.0001
298.15	7.5124	0.024	0.8826	0.0001
303.15	6.5639	0.021	0.8790	0.00006
308.15	5.7810	0.017	0.8753	0.0001
313.15	5.1287	0.017	0.8717	0.0001
318.15	4.5795	0.016	0.8681	0.00006
323.15	4.1139	0.014	0.8645	0.00006
328.15	3.7142	0.012	0.8609	0.00006
333.15	3.3704	0.013	0.8573	0.00006
338.15	3.0724	0.012	0.8537	0.00006
343.15	2.8083	0.0049	0.8500	0
348.15	2.5788	0.0022	0.8464	0
353.15	2.3777	0.0015	0.8428	0
358.15	2.2004	0.0013	0.8392	0
363.15	2.0426	0.0012	0.8356	0.00006

Table B8 – ln(η_{mixt}) for binary and ternary mixture of biodiesels.

	B50 Soybean+B50 Rapeseed			B50 Soybean+B50 Palm			B50 Rapeseed+B50 Palm			Ternary Mixture		
T/ K	Exp	Pred	Er / %	Exp	Pred	Er / %	Exp	Pred	Er / %	Exp	Pred	Er / %
283.15	2.42	2.42	-0.10									
288.15	2.26	2.26	-0.14									
293.15	2.11	2.11	-0.13	2.20	2.21	-0.64	2.14	2.14	0.080	2.16	2.15	0.24
298.15	1.97	1.97	-0.11	2.05	2.06	-0.62	2.00	2.00	0.070	2.02	2.01	0.28
303.15	1.84	1.84	-0.080	1.92	1.93	-0.57	1.86	1.86	0.13	1.88	1.88	0.29
308.15	1.71	1.71	-0.080	1.79	1.80	-0.55	1.74	1.73	0.11	1.75	1.75	0.31
313.15	1.60	1.60	-0.050	1.67	1.68	-0.54	1.61	1.61	0.11	1.63	1.63	0.33
318.15	1.49	1.49	0.070	1.55	1.56	-0.48	1.50	1.50	0.13	1.52	1.52	0.41
323.15	1.38	1.38	0.17	1.45	1.45	-0.43	1.39	1.39	0.17	1.41	1.41	0.50
328.15	1.28	1.28	0.26	1.34	1.35	-0.37	1.29	1.29	0.24	1.31	1.30	0.56
333.15	1.19	1.18	0.45	1.24	1.25	-0.32	1.19	1.19	0.30	1.22	1.21	0.71
338.15	1.10	1.09	0.56	1.15	1.15	-0.38	1.10	1.10	0.35	1.12	1.11	0.80
343.15	1.01	1.00	0.70	1.06	1.06	-0.33	1.01	1.01	0.39	1.03	1.02	0.75
348.15	0.93	0.92	0.95	0.98	0.98	-0.11	0.93	0.92	0.49	0.95	0.94	0.87
353.15	0.85	0.84	1.3	0.89	0.89	0.18	0.84	0.84	0.55	0.87	0.86	1.1
358.15	0.77	0.76	1.7	0.82	0.81	0.85	0.77	0.76	0.60	0.79	0.78	1.4
363.15	0.70	0.69	2.1	0.75	0.74	1.3	0.69	0.69	0.68	0.71	0.70	1.6

Table B9–Densisites of binary and ternary mixture of biodiesels, in g.cm^{-3}.

	B50 Soybean+B50 Rapeseed			B50 Soybean+B50 Palm			B50 Rapeseed+B50 Palm			Ternary Mixture		
T/ K	Exp	Pred	Er / %	Exp	Pred	Er / %	Exp	Pred	Er / %	Exp	Pred	Er / %
283.15	0.8963	0.8951	0.1									
288.15	0.8926	0.8914	0.1									
293.15	0.8890	0.8877	0.1	0.8868	0.8861	0.07	0.8835	0.8830	0.05	0.8862	0.8856	0.07
298.15	0.8853	0.8841	0.1	0.8831	0.8825	0.07	0.8798	0.8794	0.05	0.8826	0.8820	0.07
303.15	0.8816	0.8805	0.1	0.8795	0.8788	0.08	0.8762	0.8757	0.05	0.8790	0.8784	0.07
308.15	0.8780	0.8769	0.1	0.8759	0.8752	0.08	0.8725	0.8721	0.05	0.8753	0.8747	0.07
313.15	0.8744	0.8732	0.1	0.8723	0.8715	0.09	0.8689	0.8684	0.06	0.8717	0.8711	0.08
318.15	0.8708	0.8696	0.1	0.8687	0.8679	0.08	0.8652	0.8648	0.05	0.8681	0.8675	0.07
323.15	0.8671	0.8660	0.1	0.8650	0.8643	0.08	0.8616	0.8611	0.06	0.8645	0.8638	0.08
328.15	0.8635	0.8624	0.1	0.8614	0.8607	0.08	0.8580	0.8575	0.06	0.8609	0.8602	0.07
333.15	0.8599	0.8588	0.1	0.8578	0.8571	0.08	0.8543	0.8539	0.05	0.8573	0.8566	0.08
338.15	0.8563	0.8551	0.1	0.8541	0.8535	0.07	0.8507	0.8503	0.05	0.8537	0.8530	0.08
343.15	0.8527	0.8515	0.1	0.8505	0.8499	0.07	0.8471	0.8466	0.06	0.8500	0.8493	0.08
348.15	0.8491	0.8479	0.1	0.8469	0.8463	0.07	0.8435	0.8430	0.06	0.8464	0.8457	0.08
353.15	0.8455	0.8443	0.1	0.8433	0.8427	0.07	0.8399	0.8393	0.07	0.8428	0.8421	0.09
358.15	0.8419	0.8407	0.1	0.8397	0.8391	0.07	0.8363	0.8358	0.06	0.8392	0.8385	0.08
363.15	0.8383	0.8372	0.1	0.8361	0.8356	0.06	0.8327	0.8322	0.06	0.8356	0.8350	0.08

Appendix C

Table C1- Masses of biodiesel of soybean and diesel fuel used to prepared blends.

	19.99% BD + 80.01% Diesel fuel	39.91% BD + 60.09% Diesel fuel	59.86% BD + 40.14% Diesel fuel	79.83% BD + 20.17% Diesel fuel
$m_{Biodiesel}$ / g	0.8594	1.7081	2.5723	3.3657
m_{diesel} / g	3.4407	2.5713	1.725	0.8505

Table C2- Masses of biodiesel of rapeseed and diesel fuel used to prepared blends.

	19.99% BD + 80.01% Diesel fuel	39.93% BD + 60.07% Diesel fuel	59.92% BD + 40.08% Diesel fuel	79.96% BD + 20.04% Diesel fuel
$m_{Biodiesel}$ / g	0.8354	1.7205	2.5654	3.437
m_{diesel} / g	3.3434	2.5886	1.7159	0.8613

Table C3- Masses of biodiesel of palm and diesel fuel used to prepared blends.

	19.99% BD + 80.01% Diesel fuel	39.93% BD + 60.07% Diesel fuel	59.92% BD + 40.08% Diesel fuel	79.96% BD + 20.04% Diesel fuel
$m_{Biodiesel}$ / g	20.00	39.99	59.99	79.98
m_{diesel} / g	80.00	60.01	40.01	20.02

Table C4-Dynamic viscosity and density with the associated standard deviation for diesel fuel as a function of temperature.

T / K	Viscosity / mPa.s	$\sigma_{viscosity}$	Density / g.cm^{-3}	$\sigma_{Density}$
283.15	6.9238	0.15	0.8430	0.0002
288.15	5.8866	0.12	0.8395	0.0002
293.15	5.0616	0.092	0.8361	0.0002
298.15	4.3958	0.073	0.8326	0.0002
303.15	3.8492	0.057	0.8291	0.0002
308.15	3.3984	0.045	0.8257	0.0002
313.15	3.0234	0.040	0.8222	0.0001
318.15	2.7079	0.032	0.8188	0.0002
323.15	2.4393	0.027	0.8153	0.0001
328.15	2.2087	0.021	0.8118	0.0001
333.15	2.0098	0.017	0.8084	0.00006
338.15	1.8373	0.015	0.8049	0
343.15	1.6861	0.013	0.8014	0
348.15	1.5531	0.010	0.7979	0.00006
353.15	1.4357	0.0086	0.7945	0.0001
358.15	1.3313	0.0072	0.7910	0.0001
363.15	1.2384	0.0063	0.7876	0.00006

Table C5-Dynamic viscosity and density with the associated standard deviation for binary blend, biodiesel of soybean (80%) and diesel fuel (20%) as a function of temperature.

T / K	Viscosity / mPa.s	$\sigma_{viscosity}$	Density / g.cm^{-3}	$\sigma_{Density}$
283.15	10.6280	0.010	0.8870	0.0002
288.15	9.0482	0.0077	0.8834	0.0002
293.15	7.7918	0.0039	0.8797	0.0002
298.15	6.7678	0.0029	0.8761	0.0002
303.15	5.9333	0.0041	0.8725	0.0002
308.15	5.2392	0.0013	0.8690	0.0002
313.15	4.6600	0.0012	0.8654	0.0002
318.15	4.1728	0.0012	0.8618	0.0002
323.15	3.7564	0.00076	0.8582	0.0002
328.15	3.3986	0.0014	0.8546	0.0001
333.15	3.0902	0.00082	0.8511	0.0001
338.15	2.8229	0.00064	0.8475	0.0001
343.15	2.5891	0.00040	0.8440	0.00006
348.15	2.3837	0.00023	0.8404	0.0001
353.15	2.2025	0.00035	0.8369	0.0001
358.15	2.0413	0.00032	0.8334	0.0001
363.15	1.8977	0.00035	0.8298	0.0002

Table C6-Dynamic viscosity and density with the associated standard deviation for binary blend, biodiesel of soybean (60%) and diesel fuel (40%) as a function of temperature.

T / K	Viscosity / mPa.s	$\sigma_{viscosity}$	Density / g.cm^{-3}	$\sigma_{Density}$
283.15	9.4165	0.031	0.8753	0.0002
288.15	8.0235	0.026	0.8717	0.0002
293.15	6.9086	0.018	0.8681	0.0002
298.15	6.0040	0.017	0.8646	0.0002
303.15	5.2632	0.014	0.8610	0.0002
308.15	4.6514	0.011	0.8575	0.0001
313.15	4.1385	0.0087	0.8539	0.0001
318.15	3.7053	0.0068	0.8503	0.00006
323.15	3.3359	0.0051	0.8467	0.00006
328.15	3.0201	0.0047	0.8432	0.0001
333.15	2.7459	0.0044	0.8396	0.00006
338.15	2.5086	0.0041	0.8361	0.0001
343.15	2.3013	0.0035	0.8325	0.00006
348.15	2.1191	0.0030	0.8290	0.0001
353.15	1.9582	0.0024	0.8255	0.0001
358.15	1.8156	0.0022	0.8219	0.0001
363.15	1.6887	0.0020	0.8184	0.0001

Table C7-Dynamic viscosity and density with the associated standard deviation for binary blend, biodiesel of soybean (40%) and diesel fuel (60%) as a function of temperature.

T / K	Viscosity / mPa.s	$\sigma_{viscosity}$	Density / g.cm^{-3}	$\sigma_{Density}$
283.15	8.4389	0.021	0.8641	0.0001
288.15	7.1837	0.016	0.8606	0.00006
293.15	6.1876	0.012	0.8570	0.0001
298.15	5.3775	0.0099	0.8535	0.0001
303.15	4.7146	0.0081	0.8500	0.00006
308.15	4.1679	0.0068	0.8464	0.0001
313.15	3.7106	0.0053	0.8429	0.0001
318.15	3.3240	0.0044	0.8394	0.0001
323.15	2.9946	0.0038	0.8359	0.0002
328.15	2.7122	0.0032	0.8323	0.0001
333.15	2.4672	0.0025	0.8288	0.0001
338.15	2.2553	0.0020	0.8252	0.0001
343.15	2.0699	0.0015	0.8217	0.0001
348.15	1.9070	0.0012	0.8182	0.00006
353.15	1.7632	0.00099	0.8146	0.0001
358.15	1.6356	0.00095	0.8111	0.0001
363.15	1.5220	0.00095	0.8076	0.0001

Table C8-Dynamic viscosity and density with the associated standard deviation for binary blend, biodiesel of soybean (20%) and diesel fuel (80%) as a function of temperature.

T / K	Viscosity / mPa.s	$\sigma_{viscosity}$	Density / g.cm^{-3}	$\sigma_{Density}$
283.15	7.6623	0.011	0.8532	0.0002
288.15	6.5197	0.011	0.8497	0.0002
293.15	5.6045	0.0081	0.8462	0.0002
298.15	4.8676	0.0083	0.8427	0.0002
303.15	4.2653	0.0074	0.8392	0.0002
308.15	3.7677	0.0062	0.8357	0.0001
313.15	3.3519	0.0047	0.8322	0.0001
318.15	3.0008	0.0040	0.8287	0.0001
323.15	2.7019	0.0023	0.8253	0.00006
328.15	2.4463	0.0018	0.8218	0.00006
333.15	2.2257	0.0017	0.8183	0.00006
338.15	2.0344	0.0012	0.8148	0.00006
343.15	1.8671	0.0010	0.8113	0
348.15	1.7199	0.00099	0.8078	0
353.15	1.5892	0.0012	0.8043	0
358.15	1.4744	0.00091	0.8008	0
363.15	1.3715	0.00081	0.7974	0.00006

Table C9-Dynamic viscosity and density with the associated standard deviation for binary blend, biodiesel of rapeseed (80%) and diesel fuel (20%) as a function of temperature.

T / K	Viscosity / mPa.s	$\sigma_{viscosity}$	Density / g.cm^{-3}	$\sigma_{Density}$
283.15	9.5539	0.029	0.8822	0.0001
288.15	8.1493	0.024	0.8785	0.00006
293.15	7.0237	0.019	0.8749	0.0001
298.15	6.1089	0.016	0.8713	0.0001
303.15	5.3590	0.013	0.8677	0.0001
308.15	4.7386	0.011	0.8641	0.0002
313.15	4.2188	0.0088	0.8604	0.0001
318.15	3.7792	0.0072	0.8568	0.0001
323.15	3.4045	0.0058	0.8532	0.0001
328.15	3.0830	0.0050	0.8496	0.0001
333.15	2.8041	0.0043	0.8460	0.0001
338.15	2.5627	0.0038	0.8424	0.0001
343.15	2.3514	0.0033	0.8388	0.0001
348.15	2.1657	0.0029	0.8352	0.0001
353.15	2.0016	0.0024	0.8316	0.0001
358.15	1.8561	0.0020	0.8280	0.0001
363.15	1.7264	0.0019	0.8244	0.00006

Table C10-Dynamic viscosity and density with the associated standard deviation for binary blend, biodiesel of rapeseed (60%) and diesel fuel (40%) as a function of temperature.

T / K	Viscosity / mPa.s	$\sigma_{viscosity}$	Density / g.cm^{-3}	$\sigma_{Density}$
283.15	8.7232	0.016	0.8717	0.00006
288.15	7.4366	0.012	0.8681	0.00006
293.15	6.4105	0.011	0.8645	0.0001
298.15	5.5743	0.0085	0.8609	0.0001
303.15	4.8896	0.0074	0.8573	0.0001
308.15	4.3243	0.0059	0.8538	0.00006
313.15	3.8503	0.0052	0.8502	0.0001
318.15	3.4496	0.0042	0.8466	0.0001
323.15	3.1079	0.0035	0.8430	0.00006
328.15	2.8150	0.0030	0.8395	0.0001
333.15	2.5609	0.0023	0.8359	0.00006
338.15	2.3410	0.0019	0.8324	0.00006
343.15	2.1485	0.0018	0.8288	0.0001
348.15	1.9792	0.0014	0.8252	0.00006
353.15	1.8298	0.00098	0.8217	0.0001
358.15	1.6973	0.00083	0.8182	0.0001
363.15	1.5791	0.0010	0.8146	0.00006

Table C11-Dynamic viscosity and density with the associated standard deviation for binary blend, biodiesel of rapeseed (40%) and diesel fuel (60%) as a function of temperature.

T / K	Viscosity / mPa.s	$\sigma_{viscosity}$	Density / g.cm^{-3}	$\sigma_{Density}$
283.15	8.0286	0.023	0.8616	0.00006
288.15	6.8401	0.021	0.8580	0.0001
293.15	5.8881	0.018	0.8545	0.00006
298.15	5.1190	0.016	0.8510	0.00006
303.15	4.4890	0.014	0.8474	0.0001
308.15	3.9676	0.012	0.8439	0.00006
313.15	3.5312	0.011	0.8404	0.00006
318.15	3.1628	0.0094	0.8368	0.00006
323.15	2.8487	0.0081	0.8333	0
328.15	2.5799	0.0073	0.8298	0
333.15	2.3477	0.0066	0.8263	0
338.15	2.1458	0.0058	0.8227	0
343.15	1.9692	0.0048	0.8192	0
348.15	1.8139	0.0048	0.8157	0
353.15	1.6762	0.0042	0.8121	0
358.15	1.5547	0.0037	0.8086	0
363.15	1.4465	0.0035	0.8051	0

Table C12-Dynamic viscosity and density with the associated standard deviation for binary blend, biodiesel of rapeseed (20%) and diesel fuel (80%) as a function of temperature.

T / K	Viscosity / mPa.s	$\sigma_{viscosity}$	Density / g.cm^{-3}	$\sigma_{Density}$
283.15	7.5801	0.028	0.8544	0
288.15	6.4550	0.022	0.8509	0.00006
293.15	5.5530	0.018	0.8474	0.00006
298.15	4.8243	0.015	0.8439	0.00006
303.15	4.2286	0.013	0.8404	0.00006
308.15	3.7368	0.011	0.8369	0.00006
313.15	3.3251	0.0010	0.8334	0.00006
318.15	2.9778	0.0089	0.8299	0.00006
323.15	2.6825	0.0078	0.8263	0.00006
328.15	2.4295	0.0071	0.8228	0.00006
333.15	2.2105	0.0055	0.8193	0
338.15	2.0207	0.0046	0.8158	0
343.15	1.8548	0.0038	0.8123	0
348.15	1.7088	0.0036	0.8088	0
353.15	1.5791	0.0032	0.8053	0
358.15	1.4651	0.0028	0.8018	0
363.15	1.3632	0.0026	0.7983	0

Table C13-Dynamic viscosity and density with the associated standard deviation for binary blend, biodiesel of palm (80%) and diesel fuel (20%) as a function of temperature.

T / K	Viscosity / mPa.s	$\sigma_{viscosity}$	Density / g.cm^{-3}	$\sigma_{Density}$
293.15	8.3199	0.088	0.8716	0
298.15	7.1784	0.051	0.8680	0
303.15	6.2460	0.044	0.8644	0
308.15	5.4774	0.037	0.8608	0.00006
313.15	4.8424	0.032	0.8572	0.00006
318.15	4.3086	0.028	0.8536	0.00006
323.15	3.8564	0.024	0.8500	0.00006
328.15	3.4701	0.020	0.8464	0.00006
333.15	3.1358	0.012	0.8428	0
338.15	2.8461	0.0074	0.8392	0
343.15	2.5975	0.0029	0.8356	0
348.15	2.3818	0.0014	0.8320	0
353.15	2.1930	0.0012	0.8284	0
358.15	2.0263	0.0010	0.8248	0.00006
363.15	1.8786	0.0012	0.8213	0.00006

Table C14-Dynamic viscosity and density with the associated standard deviation for binary blend, biodiesel of palm (60%) and diesel fuel (40%) as a function of temperature.

T / K	Viscosity / mPa.s	$\sigma_{viscosity}$	Density / g.cm^{-3}	$\sigma_{Density}$
293.15	7.3410	0.057	0.8622	0.0002
298.15	6.3497	0.057	0.8586	0.0001
303.15	5.5320	0.050	0.8550	0.0001
308.15	4.8609	0.042	0.8515	0.0001
313.15	4.3051	0.039	0.8479	0.0001
318.15	3.8362	0.034	0.8444	0.00006
323.15	3.4378	0.026	0.8409	0.00006
328.15	3.0975	0.019	0.8373	0.00006
333.15	2.8028	0.012	0.8337	0
338.15	2.5484	0.0035	0.8302	0
343.15	2.3296	0.0010	0.8266	0
348.15	2.1393	0.00075	0.8231	0
353.15	1.9719	0.00081	0.8195	0
358.15	1.8241	0.00086	0.8160	0
363.15	1.6925	0.00064	0.8124	0

Table C15-Dynamic viscosity and density with the associated standard deviation for binary blend, biodiesel of palm (40%) and diesel fuel (60%) as a function of temperature.

T / K	Viscosity / mPa.s	$\sigma_{viscosity}$	Density / g.cm^{-3}	$\sigma_{Density}$
293.15	6.4042	0.084	0.8530	0.00006
298.15	5.5493	0.076	0.8495	0.00006
303.15	4.8452	0.061	0.8460	0.00006
308.15	4.2678	0.051	0.8424	0
313.15	3.7861	0.044	0.8389	0
318.15	3.3791	0.037	0.8354	0
323.15	3.0362	0.032	0.8319	0.00006
328.15	2.7416	0.028	0.8283	0.00006
333.15	2.4879	0.024	0.8248	0
338.15	2.2684	0.021	0.8213	0.00006
343.15	2.0771	0.018	0.8177	0.00006
348.15	1.9093	0.016	0.8142	0.00006
353.15	1.7612	0.013	0.8107	0.0001
358.15	1.6302	0.012	0.8072	0.00006
363.15	1.5132	0.0093	0.8036	0.00006

Table C16-Dynamic viscosity and density with the associated standard deviation for binary blend, biodiesel of palm (20%) and diesel fuel (80%) as a function of temperature.

T / K	Viscosity / mPa.s	$\sigma_{viscosity}$	Density / g.cm^{-3}	$\sigma_{Density}$
293.15	5.6605	0.014	0.8443	0.00006
298.15	4.9126	0.011	0.8408	0.00006
303.15	4.2995	0.0087	0.8373	0.00006
308.15	3.7943	0.0076	0.8338	0.00006
313.15	3.3734	0.0057	0.8303	0.00006
318.15	3.0181	0.0044	0.8268	0.00006
323.15	2.7160	0.0037	0.8234	0.00006
328.15	2.4575	0.0030	0.8199	0
333.15	2.2337	0.0023	0.8164	0.00006
338.15	2.0403	0.0019	0.8129	0
343.15	1.8714	0.0016	0.8094	0
348.15	1.7230	0.0013	0.8059	0.00006
353.15	1.5921	0.0010	0.8024	0.00006
358.15	1.4760	0.00082	0.7989	0
363.15	1.3725	0.00059	0.7954	0

Table C17- Masses of diesel fuel and cyclohexane for preparation of samples for obtain the calibration curve.

Sample	m_{diesel} / g	m_{cyc} /g	W_{diesel}	W_{cyc}	IR
1	0.6225	0.0364	0.94	0.06	1.4575
2	0.6050	0.0850	0.88	0.12	1.4550
3	0.5274	0.1038	0.84	0.16	1.4535
4	0.4936	0.3013	0.62	0.38	1.4440
5	0.5238	0.5049	0.51	0.49	1.4390
6	0.3554	0.5164	0.41	0.59	1.4350
7	0.1407	0.5077	0.22	0.78	1.4285
8	0.1054	0.6110	0.15	0.85	1.4265
9	0.0732	0.9339	0.07	0.93	1.4230
10	0.0351	0.6156	0.05	0.95	1.4225
11	100	0	1.00	0.00	1.4600
12	0	100	0.00	1.00	1.4195

Table C18- Properties of ciclohexane.

T_{bp}/ºC	81.1
IR	1.4195
k_b/ºC.Kg.mol^{-1}	2.79
m_i / g	4.5993

Table C19-Masses of diesel fuel introduced in ebuliometer.

Sample	m_i / g	m_f / g	m_{diesel} / g	$m_{mixture}$ / g
1	2.9688	2.3733	0.5955	5.1948
2	2.7000	2.3677	0.3323	5.5271
3	2.7897	2.3676	0.4221	5.9492
4	2.7449	2.3498	0.3951	6.3443
5	2.7389	2.3738	0.3651	6.7094

Table C20-Results obtained for boiling temperature, refractive index and massic composition of diesel fuel in mixture.

Sample	T_{bp}/ k	IR	W_{diesel} mixture
1	356.12	1.4250	0.13
2	356.69	1.4260	0.16
3	357.99	1.4315	0.29
4	359.35	1.4335	0.34
5	363.04	1.4365	0.42

Table C21–ln(η_{mixt}) for biodiesels of soybean-diesel blends.

	B20			B40			B60			B80		
T(K)	Exp	Pred	Er(%)	Exp	Pred	Er(%)	Exp	Pred	Er(%)	Exp	Pred	Er(%)
283.15	2.04	2.04	-0.36	2.13	2.15	-0.94	2.24	2.26	-0.95	2.36	2.38	-0.53
288.15	1.87	1.88	-0.36	1.97	1.99	-0.99	2.08	2.10	-0.97	2.20	2.22	-0.58
293.15	1.72	1.73	-0.42	1.82	1.84	-0.99	1.93	1.95	-0.99	2.05	2.06	-0.56
298.15	1.58	1.59	-0.44	1.68	1.70	-1.0	1.79	1.81	-1.0	1.91	1.92	-0.58
303.15	1.45	1.46	-0.44	1.55	1.57	-1.0	1.66	1.68	-1.0	1.78	1.79	-0.57
308.15	1.33	1.33	-0.43	1.43	1.44	-1.0	1.54	1.55	-1.0	1.66	1.67	-0.57
313.15	1.21	1.22	-0.46	1.31	1.32	-1.0	1.42	1.44	-1.1	1.54	1.55	-0.57
318.15	1.10	1.10	-0.48	1.20	1.21	-0.98	1.31	1.32	-1.0	1.43	1.43	-0.43
323.15	0.99	1.00	-0.53	1.10	1.11	-0.97	1.20	1.22	-1.0	1.32	1.33	-0.36
328.15	0.89	0.90	-0.54	1.00	1.01	-0.95	1.11	1.12	-1.0	1.22	1.23	-0.31
333.15	0.80	0.80	-0.52	0.90	0.91	-0.91	1.01	1.02	-0.95	1.13	1.13	-0.11
338.15	0.71	0.71	-0.55	0.81	0.82	-0.92	0.92	0.93	-0.98	1.04	1.04	-0.03
343.15	0.62	0.63	-0.55	0.73	0.73	-0.91	0.83	0.84	-0.98	0.95	0.95	0.07
348.15	0.54	0.54	-0.50	0.65	0.65	-0.76	0.75	0.76	-0.83	0.87	0.87	0.37
353.15	0.46	0.47	-0.46	0.57	0.57	-0.49	0.67	0.68	-0.56	0.79	0.78	0.85
358.15	0.39	0.39	-0.17	0.49	0.49	-0.09	0.60	0.60	-0.13	0.71	0.70	1.5
363.15	0.32	0.32	0.020	0.42	0.42	0.32	0.52	0.52	0.23	0.64	0.63	2.0

Table C22–Densisites of biodiesel of soybean-diesel blends, in g.cm^{-3}.

	B20			B40			B60			B80		
T / K	Exp	Pred	Er / %	Exp	Pred	Er / %	Exp	Pred	Er / %	Exp	Pred	Er / %
283.15	0.8532	0.8540	-0.1	0.8641	0.8650	-0.1	0.8753	0.8760	-0.08	0.8870	0.8870	-0.003
288.15	0.8497	0.8505	-0.1	0.8606	0.8614	-0.1	0.8717	0.8724	-0.08	0.8834	0.8834	0.0001
293.15	0.8462	0.8470	-0.1	0.8570	0.8579	-0.1	0.8681	0.8689	-0.08	0.8797	0.8798	-0.008
298.15	0.8427	0.8435	-0.1	0.8535	0.8544	-0.1	0.8646	0.8653	-0.08	0.8761	0.8762	-0.01
303.15	0.8392	0.8400	-0.1	0.8500	0.8509	-0.1	0.8610	0.8617	-0.08	0.8725	0.8726	-0.009
308.15	0.8357	0.8366	-0.1	0.8464	0.8474	-0.1	0.8575	0.8582	-0.09	0.8690	0.8690	-0.009
313.15	0.8322	0.8330	-0.1	0.8429	0.8438	-0.1	0.8539	0.8546	-0.09	0.8654	0.8654	-0.008
318.15	0.8287	0.8296	-0.1	0.8394	0.8403	-0.1	0.8503	0.8511	-0.09	0.8618	0.8619	-0.01
323.15	0.8253	0.8261	-0.1	0.8359	0.8368	-0.1	0.8467	0.8475	-0.09	0.8582	0.8583	-0.006
328.15	0.8218	0.8226	-0.1	0.8323	0.8333	-0.1	0.8432	0.8440	-0.1	0.8546	0.8548	-0.01
333.15	0.8183	0.8191	-0.1	0.8288	0.8298	-0.1	0.8396	0.8405	-0.1	0.8511	0.8512	-0.01
338.15	0.8148	0.8156	-0.1	0.8252	0.8262	-0.1	0.8361	0.8369	-0.1	0.8475	0.8476	-0.008
343.15	0.8113	0.8121	-0.1	0.8217	0.8227	-0.1	0.8325	0.8333	-0.1	0.8440	0.8440	-0.003
348.15	0.8078	0.8086	-0.1	0.8182	0.8192	-0.1	0.8290	0.8298	-0.1	0.8404	0.8404	-0.002
353.15	0.8043	0.8051	-0.1	0.8146	0.8157	-0.1	0.8255	0.8262	-0.1	0.8369	0.8368	0.003
358.15	0.8008	0.8016	-0.1	0.8111	0.8122	-0.1	0.8219	0.8228	-0.1	0.8334	0.8333	0.002
363.15	0.7974	0.7982	-0.1	0.8076	0.8087	-0.1	0.8184	0.8193	-0.1	0.8298	0.8299	-0.008

Table C23– ln(η_{mixt}) for biodiesels of rapeseed-diesel blends.

	B20			B40			B60			B80		
T / K	Exp	Pred	Er / %	Exp	Pred	Er / %	Exp	Pred	Er / %	Exp	Pred	Er / %
283.15	2.03	2.02	0.50	2.08	2.10	-0.65	2.17	-0.61	-0.61	2.26	2.26	-0.28
288.15	1.86	1.85	0.60	1.92	1.94	-0.67	2.01	-0.63	-0.63	2.10	2.10	-0.28
293.15	1.71	1.70	0.65	1.77	1.79	-0.71	1.86	-0.62	-0.62	1.95	1.95	-0.27
298.15	1.57	1.56	0.72	1.63	1.65	-0.74	1.72	-0.64	-0.64	1.81	1.81	-0.27
303.15	1.44	1.43	0.83	1.50	1.51	-0.75	1.59	-0.65	-0.65	1.68	1.68	-0.27
308.15	1.32	1.31	0.96	1.38	1.39	-0.78	1.46	-0.65	-0.65	1.56	1.56	-0.27
313.15	1.20	1.19	1.1	1.26	1.27	-0.84	1.35	-0.66	-0.66	1.44	1.44	-0.27
318.15	1.09	1.08	1.2	1.15	1.16	-0.91	1.24	-0.69	-0.69	1.33	1.33	-0.27
323.15	0.99	0.97	1.3	1.05	1.06	-1.0	1.13	-0.74	-0.74	1.23	1.23	-0.28
328.15	0.89	0.87	1.5	0.95	0.96	-1.1	1.03	-0.76	-0.76	1.13	1.13	-0.28
333.15	0.79	0.78	1.7	0.85	0.86	-1.2	0.94	-0.84	-0.84	1.03	1.03	-0.32
338.15	0.70	0.69	1.9	0.76	0.77	-1.3	0.85	-0.91	-0.91	0.94	0.94	-0.35
343.15	0.62	0.60	2.2	0.68	0.69	-1.5	0.76	-0.98	-0.98	0.86	0.86	-0.37
348.15	0.54	0.52	2.6	0.60	0.61	-1.6	0.68	-1.03	-1.0	0.77	0.78	-0.37
353.15	0.46	0.44	3.0	0.52	0.53	-1.9	0.60	-1.11	-1.1	0.69	0.70	-0.41
358.15	0.38	0.37	3.7	0.44	0.45	-2.2	0.53	-1.17	-1.2	0.62	0.62	-0.41
363.15	0.31	0.30	4.5	0.37	0.38	-2.5	0.46	-1.25	-1.3	0.55	0.55	-0.41

Table C24–Densisites of biodiesel of rapeseed-diesel blends, in g.cm^{-3}.

	B20			B40			B60			B80		
T / K	Exp	Pred	Er / %	Exp	Pred	Er / %	Exp	Pred	Er / %	Exp	Pred	Er / %
283.15	0.8544	0.8528	0.2	0.8616	0.8625	-0.1	0.8717	0.8723	-0.08	0.8822	0.8821	0.007
288.15	0.8509	0.8493	0.2	0.8580	0.8590	-0.1	0.8681	0.8687	-0.08	0.8785	0.8785	0.001
293.15	0.8474	0.8458	0.2	0.8545	0.8554	-0.1	0.8645	0.8651	-0.08	0.8749	0.8749	0.003
298.15	0.8439	0.8423	0.2	0.8510	0.8519	-0.1	0.8609	0.8616	-0.08	0.8713	0.8713	-0.0002
303.15	0.8404	0.8388	0.2	0.8474	0.8484	-0.1	0.8573	0.8580	-0.08	0.8677	0.8677	0.001
308.15	0.8369	0.8353	0.2	0.8439	0.8449	-0.1	0.8538	0.8545	-0.08	0.8641	0.8641	-0.002
313.15	0.8334	0.8318	0.2	0.8404	0.8413	-0.1	0.8502	0.8509	-0.08	0.8604	0.8605	-0.004
318.15	0.8299	0.8283	0.2	0.8368	0.8378	-0.2	0.8466	0.8473	-0.09	0.8568	0.8569	-0.007
323.15	0.8263	0.8248	0.2	0.8333	0.8343	-0.1	0.8430	0.8438	-0.09	0.8532	0.8533	-0.01
328.15	0.8228	0.8213	0.2	0.8298	0.8307	-0.1	0.8395	0.8402	-0.09	0.8496	0.8497	-0.01
333.15	0.8193	0.8178	0.2	0.8263	0.8272	-0.1	0.8359	0.8366	-0.08	0.8460	0.8461	-0.01
338.15	0.8158	0.8143	0.2	0.8227	0.8237	-0.1	0.8324	0.8331	-0.08	0.8424	0.8425	-0.01
343.15	0.8123	0.8108	0.2	0.8192	0.8201	-0.1	0.8288	0.8295	-0.08	0.8388	0.8389	-0.01
348.15	0.8088	0.8073	0.2	0.8157	0.8165	-0.1	0.8252	0.8259	-0.08	0.8352	0.8352	-0.005
353.15	0.8053	0.8037	0.2	0.8121	0.8130	-0.1	0.8217	0.8223	-0.07	0.8316	0.8316	-0.004
358.15	0.8018	0.8003	0.2	0.8086	0.8095	-0.1	0.8182	0.8188	-0.07	0.8280	0.8281	-0.008
363.15	0.7983	0.7968	0.2	0.8051	0.8060	-0.1	0.8146	0.8153	-0.08	0.8244	0.8245	-0.01

Table C25– ln(η_{mixt}) for biodiesels of palm diesel blends.

	B20			B40			B60			B80		
T / K	Exp	Pred	Er / %	Exp	Pred	Er / %	Exp	Pred	Er / %	Exp	Pred	Er / %
293.15	1.73	1.74	-0.64	1.86	1.87	-0.58	1.99	1.99	0.12	2.12	2.11	0.20
298.15	1.59	1.60	-0.64	1.71	1.72	-0.58	1.85	1.85	0.16	1.97	1.97	0.19
303.15	1.46	1.47	-0.63	1.58	1.59	-0.62	1.71	1.71	0.15	1.83	1.83	0.20
308.15	1.33	1.34	-0.61	1.45	1.46	-0.62	1.58	1.58	0.15	1.70	1.70	0.17
313.15	1.22	1.22	-0.60	1.33	1.34	-0.66	1.46	1.46	0.17	1.58	1.57	0.18
318.15	1.10	1.11	-0.61	1.22	1.23	-0.75	1.34	1.34	0.16	1.46	1.46	0.17
323.15	1.00	1.01	-0.62	1.11	1.12	-0.78	1.23	1.23	0.11	1.35	1.35	0.16
328.15	0.90	0.90	-0.62	1.01	1.02	-0.85	1.13	1.13	0.060	1.24	1.24	0.12
333.15	0.80	0.81	-0.64	0.91	0.92	-0.92	1.03	1.03	-0.040	1.14	1.14	0.050
338.15	0.71	0.72	-0.65	0.82	0.83	-1.0	0.94	0.94	-0.19	1.05	1.05	-0.11
343.15	0.63	0.63	-0.64	0.73	0.74	-1.1	0.85	0.85	-0.24	0.95	0.96	-0.20
348.15	0.54	0.55	-0.59	0.65	0.65	-1.2	0.76	0.76	-0.19	0.87	0.87	-0.18
353.15	0.47	0.47	-0.55	0.57	0.57	-1.4	0.68	0.68	-0.15	0.79	0.79	-0.15
358.15	0.39	0.39	-0.50	0.49	0.50	-1.6	0.60	0.60	-0.14	0.71	0.71	-0.17
363.15	0.32	0.32	-0.43	0.41	0.42	-1.9	0.53	0.53	-0.14	0.63	0.63	-0.16

Table C26–Densisites of biodiesel of palm-diesel blends, in g.cm^{-3}.

	B20			B40			B60			B80		
T / K	Exp	Pred	Er / %	Exp	Pred	Er / %	Exp	Pred	Er / %	Exp	Pred	Er / %
293.15	0.8443	0.8451	-0.1	0.8530	0.8542	-0.1	0.8622	0.8633	-0.1	0.8716	0.8724	-0.09
298.15	0.8408	0.8416	-0.1	0.8495	0.8507	-0.1	0.8586	0.8597	-0.1	0.8680	0.8687	-0.08
303.15	0.8373	0.8381	-0.1	0.8460	0.8471	-0.1	0.8550	0.8561	-0.1	0.8644	0.8651	-0.08
308.15	0.8338	0.8347	-0.1	0.8424	0.8436	-0.1	0.8515	0.8526	-0.1	0.8608	0.8615	-0.09
313.15	0.8303	0.8311	-0.1	0.8389	0.8400	-0.1	0.8479	0.8489	-0.1	0.8572	0.8578	-0.08
318.15	0.8268	0.8276	-0.1	0.8354	0.8365	-0.1	0.8444	0.8454	-0.1	0.8536	0.8543	-0.08
323.15	0.8234	0.8241	-0.1	0.8319	0.8330	-0.1	0.8409	0.8418	-0.1	0.8500	0.8506	-0.08
328.15	0.8199	0.8206	-0.1	0.8283	0.8294	-0.1	0.8373	0.8382	-0.1	0.8464	0.8470	-0.08
333.15	0.8164	0.8171	-0.1	0.8248	0.8259	-0.1	0.8337	0.8347	-0.1	0.8428	0.8435	-0.08
338.15	0.8129	0.8137	-0.1	0.8213	0.8224	-0.1	0.8302	0.8312	-0.1	0.8392	0.8399	-0.084
343.15	0.8094	0.8101	-0.09	0.8177	0.8188	-0.1	0.8266	0.8276	-0.1	0.8356	0.8363	-0.08
348.15	0.8059	0.8066	-0.09	0.8142	0.8153	-0.1	0.8231	0.8240	-0.1	0.8320	0.8327	-0.08
353.15	0.8024	0.8031	-0.1	0.8107	0.8118	-0.1	0.8195	0.8205	-0.1	0.8284	0.8291	-0.09
358.15	0.7989	0.7996	-0.1	0.8072	0.8083	-0.1	0.8160	0.8169	-0.1	0.8248	0.8255	-0.09
363.15	0.7954	0.7962	-0.1	0.8036	0.8048	-0.1	0.8124	0.8134	-0.1	0.8213	0.8220	-0.09

Appendix D

Table D1- Composition (wt%) and Cps of the biodiesel BDA, BDB e BDC.[82]

	BDA	BDB	BDC
C16:0	16.18	5.59	11.04
C18:0	3.82	2.39	4.07
C18:1	28.80	55.20	22.92
C18:2	50.46	34.89	61.03
CP (K)	280	271	276

Table D2- Composition (wt%) of the solid and liquid phases in equilibrium as function of temperature for biodiesel of soybean.

T / K	Liquid phase					Solid phase		Solid fraction
	C16:0	C18:0	C18:1	C18:2	C18:3	C16:0	C18:0	
258.15	3.54	0.37	26.29	61.40	8.40	85.65	14.35	9.61
260.65	4.37	0.53	26.38	60.85	7.87	80.26	19.74	8.79
263.15	7.16	1.93	25.03	58.23	7.65	69.22	30.78	4.69
265.65	6.63	0.80	25.83	58.73	8.00	79.92	20.08	5.51
268.15	8.40	1.78	24.85	57.21	7.76	65.70	34.30	3.00
270.65	10.48	3.11	22.73	55.24	8.44	34.23	65.77	-0.47
273.15	10.75	3.31	22.68	55.31	7.96	63.37	36.63	-0.35
275.65	10.85	3.31	22.68	55.23	7.93	92.81	7.19	-0.49
278.15	10.93	3.32	22.70	55.35	7.71	85.27	14.73	-0.27
280.65	9.45	2.62	23.00	55.95	8.98	71.39	28.61	0.80

Table D3- Composition (wt%) of the solid and liquid phases in equilibrium as function of temperature for biodiesel of rapeseed.

T / K	Liquid phase					Solid phase		Solid fraction
	C16:0	C18:0	C18:1	C18:2	C18:3	C16:0	C18:0	
258.15	3.09	0.59	66.77	22.38	7.17	75.36	24.64	0.04
260.65	4.50	1.02	65.22	22.03	7.23	89.21	10.79	0.05
263.15	4.98	0.83	64.58	22.51	7.11	43.89	56.11	0.03
265.65	5.31	1.54	64.26	21.71	7.18	137.06	-37.06	0.04
268.15	5.71	0.72	64.50	22.20	6.87	-72.85	172.85	0.00
270.65	4.80	0.86	64.93	22.39	7.03	60.42	39.58	0.02

Table D4- Composition (wt%) of the solid and liquid phases in equilibrium as function of temperature for biodiesel of palm.

T / K	Liquid phase					Solid phase		Solid fraction
	C16:0	C18:0	C18:1	C18:2	C18:3	C16:0	C18:0	
278.15	23.97	3.61	59.36	12.82	0.24	92.64	7.36	0.25
280.65	29.69	4.10	53.73	11.98	0.50	93.95	6.05	0.17
283.15	26.51	3.64	56.86	12.84	0.14	94.04	5.96	0.22
285.65	40.38	3.75	45.76	9.96	0.15	42.84	57.16	0.03
288.15	40.42	3.71	45.74	9.97	0.15	72.56	27.44	0.03

Table D5- Composition (wt%) of the solid and liquid phases in equilibrium as function of temperature for BDA.[82]

T / K	Liquid phase				Solid phase		Solid fraction
	C16:0	C18:0	C18:1	C18:2	C16:0	C18:0	
265.65	4.57	1.05	33.82	59.54	81.08	18.92	15.28
268.15	5.23	1.06	33.84	59.10	80.23	19.77	14.95
270.65	6.60	1.43	33.19	57.95	80.21	19.79	13.47
273.15	8.34	1.86	31.98	56.77	80.91	19.09	11.15
275.65	10.91	2.75	30.91	54.42	82.61	17.39	7.47

Table D6- Composition (wt%) of the solid and liquid phases in equilibrium as function of temperature for BDB.[82]

T / K	Liquid phase				Solid phase		Solid fraction
	C16:0	C18:0	C18:1	C18:2	C16:0	C18:0	
260.65	2.63	0.87	58.45	37.06	65.90	34.10	5.62
263.15	3.58	1.21	57.33	36.39	62.04	37.96	3.83
265.65	4.11	1.58	57.04	36.29	64.54	35.46	3.44
268.15	5.52	2.22	55.6	35.02	36.45	63.55	2.45
270.15	5.32	2.19	56.39	34.76	10.97	89.03	2.11

Table D7- Composition (wt%) of the solid and liquid phases in equilibrium as function of temperature for BDC.[82]

T / K	Liquid phase				Solid phase		Solid fraction
	C16:0	C18:0	C18:1	C18:2	C16:0	C18:0	
260.65	4.20	1.23	25.86	68.71	71.86	28.14	11.05
263.15	5.61	1.84	25.32	66.87	71.92	28.08	9.14
265.65	6.00	1.98	25.07	66.34	70.98	29.02	8.23
268.15	6.73	2.35	24.94	65.46	72.18	27.82	7.19
270.65	10.70	3.95	22.97	61.40	71.27	28.73	0.50